Upgrading a linear controller to a sliding mode one: Theory and experiments

Gabriele Perozzi, Andrey Polyakov, Felix Miranda-Villatoro, Bernard Brogliato

Upgrading a Linear Controller to a Sliding Mode One: Theory and Experiments

Gabriele Perozzi*, Andrey Polyakov, Félix Miranda-Villatoro, Bernard Brogliato

G. Perozzi and A.Polyakov are with Univ. Lille, INRIA, Centrale Lille, CNRS, UMR 9189 - CRIStAL, F-59000 Lille, France.
F. Miranda-Villatoro and B. Brogliato are with Univ. Grenoble Alpes, INRIA, CNRS, LJK, Grenoble INP, 38000 Grenoble, France.
Corresponding author * e-mail: gabriele.perozzi@inria.fr
Conflict of interest - none declared.

This work was funded by the Agence Nationale de la Recherche, project DigitSlid ANR–18-CE40-0008-01.

Abstract

This article proposes a procedure for upgrading a linear proportional controller to a sliding mode one preventing a degradation of a control quality. Two nonlinear algorithms are studied in this context: Unit and Homogeneous Sliding Mode Controllers (SMCs). The parameters of the nonlinear controllers are defined using the gains of the (already well-tuned) linear controller. The main idea of this upgrading procedure is to split the state-space into two regions, the region of the linear control and the region of the nonlinear control. This is done *via* a suitable design parameter. The theoretical developments are validated experimentally on a rotary inverted pendulum. Comparisons between the already well-tuned linear controller and the proposed upgraded nonlinear controllers are presented. The experiments in a rotary inverted pendulum demonstrate that the upgraded controller significantly improves the control precision without degradation of the control signal.

1 Introduction

A sliding mode controller (SMC) is a nonlinear set-valued control law, which is, theoretically, insensitive to the so-called matched perturbations and consequently, guarantees better control precision [1, 2, 3], as well as finite-time convergence [4, 5, 6, 7]. However, the chattering phenomenon does not allow the ideal sliding mode to be realized in practice. This may imply a degradation of the control precision instead of the promised improvement. Several methods for the chattering analysis and chattering reduction can be found in the literature, depending on its origin (unmodelled dynamics, discretization method)

[1, 8, 9, 10, 11, 12]. However, the chattering problem is still of interest [13, 14], in particular the numerical chattering that is due solely to the discretization method [11, 15].

On the other hand, linear controllers are the most popular industrial solution for feedback control. Linear control is supported by many methods of control parameters tuning in both frequency and time domains (see, *e.g.*, [16, 17]). Linear control laws provide a satisfactory performance in many applications. In this article the following question is tackled: *Is it possible to upgrade (transform) an already tuned linear controller to a sliding mode controller, with a guaranteed improvement of the control quality?* More precisely, we want to design an SMC algorithm, the quality of which could not be worse than the control quality of the linear feedback. There exists methods to design controllers with nonlinear and/or linear dynamics. However to the best of the authors' knowledge it is the first time that a rigorous procedure is proposed to upgrade a linear controller to a nonlinear one preventing a degradation of the performances. The control quality can be estimated through numerical simulations or performing experiments on a setup. It may include various indexes, which correspond to trajectory tracking precision, energetic optimality, chattering effects, input magnitude, *etc.*

The methods presented in this article assume that a linear stabilizing feedback is already designed for the system. This linear control is modified only in a certain zone of the state space in such a way that an SMC is derived. Two SMCs are considered: the unit SMC [1] and the generalized homogeneous SMC [18]. In both cases, the SMC is obtained from a linear one, and it does not need a design of all SMC parameters.

Most popular methods of SMC design are based on continuous-time models of control systems. However, even in the case of a linear control law, improper implementation of the controller in a digital device may lead to serious degradation of the control quality or even to instability of the closed-loop system (see, *e.g.*, [19]). For nonlinear control laws the situation can be even worse. For example, the conventional (the so-called Euler explicit) digital implementation of SMCs leads to the so-called numerical chattering [11] or even to a finite-time blow-up of the closed-loop system [20, 21].

Three discretization methods are proposed and compared in this article, through real experiments on a rotary inverted pendulum. The first one is the explicit (or conventional) scheme. The main issue with the explicit discretization is that it lacks of a selection calculation process for the set-valued input[1], yielding strong numerical chattering and bang-bang inputs. In order to cope with this issue it is often suggested [1] to replace the sign function by a linear saturation. The parameter of the saturation function usually is tuned for the concrete application, and tuning may not be an easy task even for simple systems [22]. The second scheme is based on the so-called implicit discretization algorithms developed in [21, 15, 23, 24, 25] for differential inclusions, see [26] for a survey. This scheme automatically computes a selection of the set-valued term.

[1]Here the word selection refers to the selection of the set-valued, or multivalued, right-hand side of a differential inclusion.

Consequently, it allows to reject the so-called numerical chattering of set-valued SMC algorithms at both the output and the input (no longer any bang-bang-like input signals), and keeps most of the nice features of the continuous-time SMC (Lyapunov stability, finite-time convergence, insensitivity to control gain during the sliding phase), even for attractive surfaces of co-dimension larger than one. This is obtained at the price, however, of using a specific online solver to compute the input. Experimental validations of these facts can be found in [21, 27, 22, 28, 29, 24]. The third method is a semi-implicit discretization, somewhat intermediate between the implicit and the explicit ones. The experiments for the rotary inverted pendulum show that all three implementations of the SMC give better control quality than the linear feedback.

The problem to be discussed is formulated in Section 2. An introduction to the homogeneous control systems is given Section 3. The procedures to design SMCs, starting from an existing linear controller, are presented in Section 4. Section 5 is dedicated to the digital implementations procedures and the consequent chattering reduction of SMC. The experiments, with comparison between the already well-tuned linear controller (provided by the manufacturer) and the proposed upgraded nonlinear controllers, are presented in Section 6. Section 7 concludes the article.

Notation. Given a square matrix P, $\lambda_{\max}(P)$ denotes its maximal eigenvalue. The graph of a set-valued mapping $\mathbf{N} : \mathbb{R}^n \rightrightarrows \mathbb{R}^m$ is the set $\{(x, y) \in \mathbb{R}^n \times \mathbb{R}^m \mid x \in \mathrm{dom}(\mathbf{N}),\ y \in \mathbf{N}(x)\}$. It is denoted as $\mathrm{Grph}(\mathbf{N})$. In the discrete-time setting, the value of the function $f(\cdot)$ at an instant t_k is denoted as $f_k \triangleq f(t_k)$. The $n \times n$ identity matrix is denoted as I_n. A function $\sigma : [0, +\infty) \to [0, +\infty)$ belongs to the class $\mathcal{K}^\infty$ if it is continuous, strictly increasing, $\sigma(0) = 0$ and $\sigma(s) \to +\infty$ as $s \to +\infty$.

2 Problem Statement

Let us consider the problem of stabilization of the linear plant

$$\dot{x} = Ax + Bu + f(t, x), \quad t \geq 0, \tag{1}$$

where $x(t) \in \mathbb{R}^n$ is the system's state, $u(t) \in \mathbb{R}^m$ is the control input, $A \in \mathbb{R}^{n\times n}$ and $B \in \mathbb{R}^{n\times m}$ are system matrices assumed to be known, and the function $f : \mathbb{R}\times\mathbb{R}^n \to \mathbb{R}^n$ describes the system's uncertainties and disturbances. The pair $\{A, B\}$ is controllable. The whole state x is assumed to be available (measured or observed) and the system is already controlled by a linear feedback

$$u_{lin} = K_{lin}x, \quad K_{lin} \in \mathbb{R}^{m\times n}. \tag{2}$$

Various schemes are developed for tuning the control gain K_{lin} (see, *e.g.*, [16]). We assume that K_{lin} is already well-tuned such that it stabilizes at least the linear (unperturbed) system (1) at zero. On the one hand, it is well-known (see, *e.g.*, [30]) that the linear controller is robust with respect to some Lipschitz

non-linearities. For example, the system (1) (2) remains globally asymptotically stable provided that $f(\cdot,\cdot)$ satisfies the inequality

$$\|f(t,x)\| \leq \eta\|x\|, \quad \forall t \in \mathbb{R}, \forall x \in \mathbb{R}^n,$$

and $\eta \geq 0$ is sufficiently small. The latter means that $f(t,x)$ has to vanish at $x = 0$. On the other hand, a SMC stabilizes the origin of the system (1) and completely rejects the so-called matched perturbations, whenever the mismatched perturbations satisfy suitable assumptions (see, *e.g.*, [1] and [18]). In the case of the classical SMC, the mentioned condition can be formalized as follows:

$$\|f(t,x) - BCf(t,x)\| \leq \eta\|x\|, \quad \forall t \in \mathbb{R}, \forall x \in \mathbb{R}^n, \tag{3}$$

where $\eta \geq 0$ is sufficiently small, and the matrix $C \in \mathbb{R}^{m\times n}$ defines the sliding surface $\{x \in \mathbb{R}^n \mid Cx = 0\}$ of a SMC system such that $CB = I_m$.

The inequality (3) means that the function $f(\cdot,\cdot)$ may have non-vanishing components at $x = 0$, which belong to the range of B (matched perturbations). Therefore, SMCs indeed reject a larger class of perturbations. In practice, the function $f(\cdot,\cdot)$ is unknown. Thus, the quality of controllers can only be validated with real experiments. Moreover, due to the chattering phenomenon, the implementation of a SMC may not guarantee a better quality of regulation than the linear one if the chattering issue is disregarded. The main goal of this work is to develop a method for upgrading a linear controller to a SMC with an improved control quality. If the system has disturbances, which is always the case in experiments, the upgraded SMC should bring also a better robustness with respect to the existing linear controller. For the classical SMC design, starting from an existing linear feedback, the following assumption is needed.

Assumption 1 *The matrix of the closed-loop linear system $A + BK_{lin}$ is Hurwitz and there exist $\Theta \in \mathbb{R}^{m\times n}$ and $\Lambda \in \mathbb{R}^{m\times m}$ such that*

$$\Theta(A + BK_{lin}) = \Lambda\Theta, \quad \Lambda + \Lambda^\top \prec 0, \tag{4}$$

such that

$$\det(\Theta B) \neq 0, \quad \Lambda\Theta B = \Theta B\Lambda. \tag{5}$$

In the case of a transformation of the linear controller to a generalized homogeneous SMC (see Section 4.2), the latter assumption can be relaxed as follows : $A + BK_{lin}$ is Hurwitz.

Notice that the conditions (4) and (5) are rather restrictive in the general case. However, they need to be fulfilled if the whole control is planned to be upgraded (transformed to a SMC). In fact, a linear feedback $\tilde{u}_{lin} = \tilde{K}_{lin}x, \tilde{K} \in \mathbb{R}^{\tilde{m}\times n}$ for the system

$$\dot{x} = \tilde{A}x + \tilde{B}\tilde{u}, \quad \tilde{A} \in \mathbb{R}^{n\times n}, \quad \tilde{B} \in \mathbb{R}^{n\times\tilde{m}}, \quad \tilde{u} \in \mathbb{R}^m \tag{6}$$

may be just partially upgraded. Indeed, selecting $1 \leq m < \tilde{m}$ and splitting the vector $\tilde{u}$ and the matrices $\tilde{B}$, $\tilde{K}_{lin}$ on blocks as follows

$$\tilde{u} = \begin{pmatrix} u \\ \hat{u} \end{pmatrix}, \quad \tilde{B} = \begin{pmatrix} B & \hat{B} \end{pmatrix}, \quad \tilde{K}_{lin} = \begin{pmatrix} K_{lin} \\ \hat{K}_{lin} \end{pmatrix}$$

$$\hat{u} \in \mathbb{R}^{\tilde{m}-m}, \quad \hat{B} \in \mathbb{R}^{n\times(\tilde{m}-m)}, \quad \hat{K}_{lin} \in \mathbb{R}^{(\tilde{m}-m)\times n},$$

we derive the system (1) (2) with

$$A = \tilde{A} + \hat{B}\hat{K}_{lin} \quad \text{and} \quad u_{lin} = K_{lin}x$$

which deals with an upgrade of the first m components of the original control $\tilde{u}_{lin}$. Assumption 1 is not very restrictive if we consider a partial or component-wise upgrade of the linear controller. Indeed, for $m = 1$ the conditions (4) and (5) simply mean that the Hurwitz matrix $A + BK_{lin}$ has at least one real eigenvalue $\Lambda < 0$ such that the corresponding left-eigenvector $\Theta \in \mathbb{R}^{1\times n} \neq 0$:

$$\Theta(A + BK_{lin}) = \Lambda\Theta$$

is not orthogonal to $B \in \mathbb{R}^n$:

$$\Theta B \neq 0.$$

This assumption holds in many practical applications.

3 Preliminaries: Generalized Homogeneity

3.1 Linear Dilations

By definition, the homogeneity is a dilation symmetry. In this paper we deal only with the so-called linear dilations [18, Chapter 6] in $\mathbb{R}^n$ given by

$$\mathbf{d}(s) = e^{sG_{\mathbf{d}}} = \sum_{i=0}^{\infty} \frac{(sG_{\mathbf{d}})^i}{i!}, \quad s \in \mathbb{R}, \tag{7}$$

where $G_{\mathbf{d}} \in \mathbb{R}^{n\times n}$ is an anti-Hurwitz matrix (i.e., the matrix $-G_{\mathbf{d}} \in \mathbb{R}^{n\times n}$ is Hurwitz), known as the *generator of the linear dilation*. The latter guarantees that $\mathbf{d}$ satisfies the limit property ($\|\mathbf{d}(s)x\| \to 0$ as $s \to -\infty$ and $\|\mathbf{d}(s)x\| \to +\infty$ as $s \to +\infty$) required for a group to be a dilation in $\mathbb{R}^n$ (see, *e.g.*, [31]). The dilation introduces an alternative norm topology in $\mathbb{R}^n$ using the so-called canonical homogeneous norm.

Definition 1 *[32] The functional $\|\cdot\|_{\mathbf{d}} : \mathbb{R}^n \to \mathbb{R}_+$ given by $\|0\|_{\mathbf{d}} = 0$ and*

$$\|x\|_{\mathbf{d}} = e^{s_x}, \quad \textit{where } s_x \in \mathbb{R} : \|\mathbf{d}(-s_x)x\| = 1, \quad x \neq 0 \tag{8}$$

is called the canonical homogeneous norm in $\mathbb{R}^n$, where $\mathbf{d}$ is a monotone dilation[2] and $\|\cdot\|$ is a norm in $\mathbb{R}^n$.

Notice that $\|x\| = 1$ (resp. $\|x\| \leq 1$) is equivalent to $\|x\|_{\mathbf{d}} = 1$ (resp. $\|x\|_{\mathbf{d}} \leq 1$). For the uniform dilation $\mathbf{d}(s) = e^s I_n, s \in \mathbb{R}$ we have $\|\cdot\| = \|\cdot\|_{\mathbf{d}}$.

[2] A dilation in $\mathbb{R}^n$ is monotone if and only if for any $x \in \mathbb{R}^n$ the function $s \to \|\mathbf{d}(s)x\|$ is monotone increasing.

Theorem 1 *[33] If* $\mathbf{d}$ *is a monotone dilation, the canonical homogeneous norm is continuous on* $\mathbb{R}^n$*, locally Lipschitz continuous on* $\mathbb{R}^n\backslash\{\mathbf{0}\}$ *and there exist* $\underline{\sigma}$, $\overline{\sigma} \in \mathcal{K}^\infty$ *such that*

$$\underline{\sigma}(\|x\|) \leq \|x\|_{\mathbf{d}} \leq \overline{\sigma}(\|x\|), \quad \forall x \in \mathbb{R}^n.$$

Moreover, $\|\cdot\|_{\mathbf{d}}$ *is differentiable on* $\mathbb{R}^n\backslash\{\mathbf{0}\}$ *provided that* $\|\cdot\|$ *is differentiable on* $\mathbb{R}^n\backslash\{\mathbf{0}\}$*. For* $\|x\| = \sqrt{x^\top P x}$ *we have*

$$\frac{\partial \|x\|_{\mathbf{d}}}{\partial x} = \|x\|_{\mathbf{d}} \frac{x^\top \mathbf{d}^\top(-\ln\|x\|_{\mathbf{d}}) P \mathbf{d}(-\ln\|x\|_{\mathbf{d}})}{x^\top \mathbf{d}^\top(-\ln\|x\|_{\mathbf{d}}) P G_{\mathbf{d}} \mathbf{d}(-\ln\|x\|_{\mathbf{d}}) x}, \quad \forall x \neq \mathbf{0}. \tag{9}$$

Below the canonical homogeneous norm is used as a Lyapunov function for analysis and design of a homogeneous SMC.

3.2 Homogeneous functions and vector fields

Definition 2 *[31] A vector field* $f : \mathbb{R}^n \to \mathbb{R}^n$ *(resp. a function* $h : \mathbb{R}^n \to \mathbb{R}$*) is said to be* $\mathbf{d}$*-homogeneous of a degree* $\mu \in \mathbb{R}$*, if* $f(\mathbf{d}(s)x) = e^{\mu s}\mathbf{d}(s)f(x)$ *(resp.* $h(\mathbf{d}(s)x) = e^{\mu s}h(x)$*), for all* $x \in \mathbb{R}^n$ *and all* $s \in \mathbb{R}$*.*

Homogeneity of a function (operator) is inherited by any other object induced by this function. For example, the Euler homogeneous function theorem implies that the derivative of the homogeneous function is homogeneous as well. If a vector field $f(\cdot)$ is $\mathbf{d}$-homogeneous of degree μ, then solutions of the ordinary differential equation (ODE):

$$\dot{x} = f(x) \tag{10}$$

are symmetric [31]:

$$x(t, \mathbf{d}(s)x_0) = \mathbf{d}(s)x(e^{\mu s}t, x_0),$$

where $x(t, z)$ denotes a solution of (10) with the initial condition $x(0) = z$.

Example 1 *[33] The linear vector field* $x \mapsto Ax$*,* $A \in \mathbb{R}^{n\times n}$ *is* $\mathbf{d}$*-homogeneous of the degree* $\mu \neq 0 \quad \Leftrightarrow \quad A$ *is nilpotent* $\quad \Leftrightarrow \quad AG_{\mathbf{d}} = (\mu I_n + G_{\mathbf{d}})A$*.*

The homogeneity degree specifies the convergence rate of the system. The following theorem can be found in [4] for the case of the so-called weighted dilation.

Theorem 2 *Let the vector field* $f : \mathbb{R}^n \to \mathbb{R}^n$ *be continuous and* $\mathbf{d}$*-homogeneous of a degree* $\nu \in \mathbb{R}$*. If the system* (10) *is asymptotically stable then it is globally*

- *finite-time stable for* $\mu < 0$*:*

$$\forall x_0 \in \mathbb{R}^n, \quad \exists T(x_0) \geq 0 : \quad \|x(t, x_0)\| = 0, \quad \forall t \geq T(x_0);$$

- *exponentially stable for* $\mu = 0$*:*

$$\exists M \geq 1, \exists \alpha > 0 : \quad \|x(t, x_0)\|_{\mathbf{d}} \leq M\|x_0\|_{\mathbf{d}} e^{\alpha t}, \quad \forall t \geq 0;$$

- *nearly fixed-time stable for $\mu > 0$:*

$$\forall r > 0, \quad \exists T_r > 0 : \quad \|x(t, x_0)\| \le r, \quad \forall t \ge T_r, \forall x_0 \in \mathbb{R}^n.$$

The homogeneous control systems are robust (input-to-state stable) with respect to a rather large class of perturbations [5, 34].

4 From Linear Control to SMC

4.1 The unit SMC

The classical concept of the SMC design for the linear plant (1) is the two-step procedure [1, 2, 3]:

1) select the sliding surface $\{x \in \mathbb{R}^n \mid Cx = 0\}$ such that the motion of the considered system on this surface is stable (all trajectories converge to zero as time goes to infinity);

2) define a control law which steers the state of (1) towards the surface $\{x \in \mathbb{R}^n \mid Cx = 0\}$ in finite time and ensures that this surface is a positively invariant set of the system (see, *e.g.*, [1] for the rigorous definition of the sliding mode).

In this article the so-called unit SMC algorithm [1] is studied. It is given by

$$u_{smc} = K_{nom} x + \gamma(t, x) \frac{Cx}{\|Cx\|}, \tag{11}$$

where $\gamma = \gamma(t, x) : \mathbb{R} \times \mathbb{R}^n \to \mathbb{R}^{m \times m}$ is such that $\lambda_{\max}(\gamma(t, x) + \gamma^\top(t, x)) < 0$,

$$K_{nom} = -(CB)^{-1} CA,$$

and the matrix $C \in \mathbb{R}^{m \times n}$ is selected such that $\det(CB) \neq 0$ and the differential-algebraic equation

$$\begin{cases} \dot{x} = (I_n - B(CB)^{-1}C)Ax, \\ Cx = 0, \end{cases} \tag{12}$$

is globally asymptotically stable. Let us denote

$$\mathbf{U}(\sigma) = \begin{cases} \frac{\sigma}{\|\sigma\|} & \text{if} \quad \|\sigma\| \neq 0 \\ \mathcal{B}_m & \text{if} \quad \|\sigma\| = 0, \end{cases}$$

where $\mathcal{B}_m$ is the unit ball in $\mathbb{R}^m$. Such a selection of the control algorithm together with the above assumptions guarantee that the differential inclusion

$$\dot{\sigma} \in \gamma(t, x)\mathbf{U}(\sigma) + Cf(t, x), \quad \sigma = Cx, \tag{13}$$

holds, securing that the surface $\{x \in \mathbb{R}^n \mid Cx = 0\}$ is a finite-time attractive invariant manifold of the closed-loop system (1) and (11), provided that

$$\sup_{t,x} \lambda_{\max} \left(\gamma(t, x) + \gamma^\top(t, x)\right) + 2\|Cf(t, x)\| < 0,$$

see [1] or the proof of Theorem 3. In the case analysed here, a linear feedback (2) is already well-tuned and provides a good performance for the closed-loop system. The objective is to make a minimal modification of the linear feedback in order to transform it to a SMC (11), and to improve the control quality.

The main idea of the upgrade can be easily explained for the single input case $m = 1$. Since, by Assumption 1, in this case the matrix of the closed-loop linear system $A + BK_{lin}$ is Hurwitz and has a real eigenvalue $\lambda < 0$, then the corresponding left eigenvector $\Theta \in \mathbb{R}^{1\times n}$ defines an invariant manifold $\Theta x = 0$ of the linear closed-loop system. This manifold is a sort of sliding surface of the linear unperturbed system, but without the finite-time attraction property yet. Therefore, for the SMC (11), the sliding surface is selected as follows:

$$Cx = 0, \quad C = (\Theta B)^{-1}\Theta. \tag{14}$$

The sliding mode control (11) is defined such that (see Fig. 1)

$$u_{smc}(x) = K_{lin}x \quad \text{for } \|Cx\| \geq \beta,$$

and for $\|Cx\| < \beta$ the SMC has the form (11), which steers all trajectories of the closed-loop system to the surface $Cx = 0$ in a finite-time. To avoid discontinuity of (11) on $\|Cx\| = \beta$ the function γ is properly selected as described below.

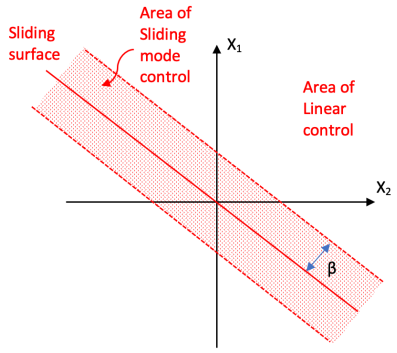

Figure 1: The illustration of the upgrade of linear control to the unit SMC.

Theorem 3 *Let the matrix $K_{lin} \in \mathbb{R}^{m\times n}$ be the gain of a linear stabilizing feedback* (2) *such that Assumption 1 holds. If*

- *the switching surface is given by* (14)*;*
- *the function $f : \mathbb{R} \times \mathbb{R}^n \to \mathbb{R}^n$ satisfies* (10) *with*

$$0 \leq \eta < \|P\|^{-1}, \tag{15}$$

and

$$\|Cf(t,x)\| \leq \rho \begin{cases} \|Cx\| & \text{if } \|Cx\| \geq \beta, \\ \beta & \text{if } \|Cx\| < \beta, \end{cases} \tag{16}$$

where $\rho \in \left[0, \frac{|\lambda_{\max}(\Lambda+\Lambda^\top)|}{2}\right)$ *is a scalar parameter and* $P = P^\top \in \mathbb{R}^{n\times n}$ *is a solution of the Lyapunov equation*

$$(A + BK_{lin})^\top P + P(A + BK_{lin}) = -2I_n, \quad P \succ 0; \tag{17}$$

- γ *is defined as follows*

$$\gamma(t,x) := \tilde{\gamma}(\|Cx\|) = \Lambda \begin{cases} \|Cx\| & \text{if} \quad \|Cx\| \geq \beta, \\ \beta & \text{if} \quad \|Cx\| < \beta, \end{cases} \tag{18}$$

where $\beta > 0$ *is a scalar parameter;*

then

1) $u_{smc} = K_{lin}x$ *for* $\|Cx\| > \beta$ *and* $Cx = 0$ *is the only discontinuity surface of* u_{smc}*;*

2) $Cx = 0$ *is the sliding surface of the closed-loop system* (1) (11) *with the following reaching-time estimate*

$$T(x(0)) \leq -2 \begin{cases} \frac{\ln\left(\frac{\|Cx(0)\|}{\beta}\right)+1}{\lambda_{\max}(\Lambda+\Lambda^\top)+2\rho} & \text{if} \quad \|Cx(0)\| > \beta \\ \frac{\|Cx(0)\|}{(\lambda_{\max}(\Lambda+\Lambda^\top)+2\rho)\beta} & \text{if} \quad \|Cx(0)\| \leq \beta; \end{cases} \tag{19}$$

3) *the closed-loop system* (1) (11) *is globally asymptotically stable.*

Proof. 1) Notice that the identities (4) and (14) imply that $C(A + BK_{lin}) = \Lambda C$, $CB = I_m$ and for $\|Cx\| \geq \beta$ we have

$$\begin{aligned} u_{smc} &= -CAx + \Lambda Cx = CBK_{lin}x - C(A + BK_{lin})x + \Lambda Cx \\ &= CBK_{lin}x - \Lambda Cx + \Lambda Cx = K_{lin}x. \end{aligned} \tag{20}$$

Hence, for $\|Cx\| \geq \beta$, it is inferred that

$$\dot{\sigma} = C(A + BK_{lin})x + Cf(t,x) = \Lambda\sigma + Cf(t,x), \tag{21}$$

where $\Lambda + \Lambda^\top \prec 0$ by Assumption 1. Moreover, the inequality (16) implies that

$$\begin{aligned} \tfrac{d\|\sigma\|^2}{dt} &= \sigma^\top(\Lambda + \Lambda^\top)\sigma + 2\sigma^\top Cf \leq \sigma^\top(\Lambda + \Lambda^\top)\sigma + 2\rho\|\sigma\|^2 \\ &= \sigma^\top(\Lambda + \Lambda^\top + 2\rho I_m)\sigma \leq (\lambda_{\max}(\Lambda + \Lambda^\top) + 2\rho)\|\sigma\|^2 < 0 \end{aligned} \tag{22}$$

for $\|\sigma\| \geq \beta$.

2) For $0 < \|Cx\| < \beta$, we have $u_{sm}(x) = -CAx + \beta\Lambda\frac{Cx}{\|Cx\|}$ and

$$\dot{\sigma} = \beta\Lambda\frac{Cx}{\|Cx\|} + Cf(t,x).$$

Hence, using the inequality (16) it is deduced that

$$\frac{d\|\sigma\|^2}{dt} \leq \beta\sigma^\top \frac{(\Lambda+\Lambda^\top)}{\|\sigma\|}\sigma + 2\beta\rho\|\sigma\| \leq \beta(\lambda_{\max}(\Lambda+\Lambda^\top)+2\rho)\|\sigma\| < 0 \quad (23)$$

for $0 < \|\sigma\| < \beta$. Combining (22) and (23) we conclude that the sliding mode in the surface $\sigma = 0$ appears in a finite time $T(x(0))$ estimated by the formula (19).

3) Recall that the equivalent control u_{eq} is the solution of the algebraic equation $CAx + CBu + Cf(t,x) = 0$ with respect to u. This equation corresponds to $\dot{\sigma} = 0$ in the sliding mode. Since $CB = I_m$ then

$$u_{eq} = -CAx - Cf(t,x).$$

For $t \geq T(x(0))$ we have $u_{smc} = u_{eq}$ (see, [35] for more details) and the dynamics of the closed-loop system is described by the differential-algebraic equation:

$$\dot{x} = Ax + Bu_{eq} + f(t,x), \quad Cx = 0.$$

Therefore, it follows that

$$\dot{x} = (A - BCA)x + f(t,x) - BCf(t,x), \quad Cx = 0.$$

Since $C(A + BK_{lin}) = \Lambda C$ and $CB = I_m$ then

$$A - BCA = A - BC(A + BK_{lin} - BK_{lin}) = A + BK_{lin} - B\Lambda C$$

and the dynamics in the sliding mode is given by

$$\dot{x} = (A + BK_{lin})x + f(t,x) - BCf(t,x), \quad Cx = 0.$$

Since $A + BK_{lin}$ is Hurwitz, there exists a positive definite solution $P = P^\top \in \mathbb{R}^{n\times n}$ to the Lyapunov equation (17). Considering the Lyapunov function candidate

$$V = x^\top Px,$$

it follows that

$$\begin{aligned}\dot{V} &= 2x^\top P(A + BK_{lin})x + 2x^\top P(f(t,x) - BCf(t,x)) \\ &\leq -2\|x\|^2 + 2\|x\|\|P(f(t,x) - BCf(t,x))\| \\ &\leq -2\|x\|(\|x\| - \|P\| \cdot \|f(t,x) - BCf(t,x)\|) < 0,\end{aligned}$$

provided that $\|f(t,x) - BCf(t,x)\| < \|P\|^{-1}\|x\|$. The proof is complete. ■

The SMC (11) (18) can be rewritten as a linear feedback with a state-dependent gain:

$$u_{smc} = K_{smc}(\|Cx\|)x \quad \text{for} \quad Cx \neq 0,$$

where $K_{smc} : (0, +\infty) \to \mathbb{R}^{m\times n}$ is defined as follows

$$K_{smc}(\varphi) = K_{nom} + \frac{\tilde{\gamma}(\varphi)}{\varphi} C, \quad \varphi > 0. \tag{24}$$

Below this representation of the SMC is used in order to introduce a chattering reduction scheme. Notice that the SMC designed by the latter theorem coincides with the linear feedback for $\|Cx\| \geq \beta$. For β tending to zero the original linear feedback is recovered. From a theoretical point of view, the larger β, the larger the magnitude of the matched perturbations to be rejected (see the formula (16)). In practice, large β may invoke large chattering magnitude, so tuning the parameter β would allow us to upgrade a linear control to a SMC and prevent a degradation of the control accuracy due to the chattering phenomenon.

Remark 1 *Theoretically, for $m = 1$ any real negative eigenvalue of the matrix $A + BK_{lin}$ satisfying Assumption 1 can be selected for the upgrade. However, in practice this selection may impact the improvement of the control quality of the obtained SMC. The best option in this case is to compare the corresponding SMCs on the experiments and select the best one, based on the desired criteria. If such a comparison is not possible, the largest negative eigenvalue (*i.e.*, closest to zero) should be selected among others.*

4.2 The generalized homogeneous SMC

The homogeneous controllers [36, 37, 5, 38, 39] are possible solutions to the considered problem. As shown in [18, Section 1.3], they may provide faster convergence, better robustness and less overshoot than linear control laws. In this paper, we consider the generalized homogeneous SMC of the form [18]:

$$u_{hom}(x) = K_0 x + K\mathbf{d}(-\ln \|x\|_{\mathbf{d}})x, \tag{25}$$

where the parameters $K_0,\ K \in \mathbb{R}^{m\times n}$, $\mathbf{d}(s) = e^{sG_{\mathbf{d}}}$, $s \in \mathbb{R}$, $G_{\mathbf{d}} \in \mathbb{R}^{n\times n}$ are defined using the following procedure:

1. Find a solution $(G_0, Y_0) \in \mathbb{R}^{n\times n} \times \mathbb{R}^{m\times n}$ of the linear equation

$$AG_0 + BY_0 = A + G_0 A, \quad G_0 B = \mathbf{0}, \tag{26}$$

and define

$$G_{\mathbf{d}} = I_n - G_0, \quad K_0 = Y_0(I_n - G_0)^{-1}; \tag{27}$$

2. Find a solution $(X, Y) \in \mathbb{R}^{n\times n} \times \mathbb{R}^{m\times n}$ of the LMI

$$\begin{cases} (A + BK_0)X + X(A + BK_0)^\top + BY + Y^\top B^\top \prec 0, \\ G_{\mathbf{d}}X + XG_{\mathbf{d}}^\top \succ 0, \quad X \succ 0 \end{cases} \tag{28}$$

and define

$$K = YX^{-1}. \tag{29}$$

The canonical homogeneous norm $\|\cdot\|_{\mathbf{d}}$ in (25) is induced by the weighted Euclidean norm

$$\|x\|_P = \sqrt{x^\top P x}, \quad P \triangleq X^{-1}.$$

In [39] it is shown that the equation (26) is always feasible provided that the pair (A, B) is controllable. The feasibility of (28) is proven in [38]. Notice that the term $\mathbf{d}(-\ln\|x\|_{\mathbf{d}})x$ is globally bounded on $\mathbb{R}^n$, continuously differentiable on $\mathbb{R}^n\backslash\{0\}$ and discontinuous at zero, since $\|\mathbf{d}(-\ln\|x\|_{\mathbf{d}})x\| = 1$ by the definition of the canonical homogeneous norm. The unperturbed closed-loop system (1), (25)

$$\dot{x} = g(x) \triangleq Ax + Bu_{hom}(x)$$

is $\mathbf{d}$-homogeneous of the degree $\mu = -1$ with the dilation $\mathbf{d}(s) = e^{sG_{\mathbf{d}}}, s \in \mathbb{R}$:

$$g(\mathbf{d}(s)x) = e^{-s}\mathbf{d}(s)g(x), \quad \forall x \neq \mathbf{0}, \quad \forall s \in \mathbb{R}$$

and it is *globally finite-time stable* with the Lyapunov function $V(x) = \|x\|_{\mathbf{d}}$ as shown below.

Proposition 1 *[18] Let the pair (A, B) be controllable, $G_{\mathbf{d}} \in \mathbb{R}^{n\times n}$, $K_0, K \in \mathbb{R}^{m\times n}$ be defined by the formulas* (26), (27), (28), (29). *If $f : \mathbb{R}\times\mathbb{R}^n\times\mathbb{R}^n$ satisfies the inequality*

$$\|x\|_{\mathbf{d}} x^\top \mathbf{d}(-\ln\|x\|_{\mathbf{d}})P\mathbf{d}(-\ln\|x\|_{\mathbf{d}})f(t,x) \leq \kappa, \tag{30}$$

for all $x \neq \mathbf{0}$ and all $t > 0$, where $P = X^{-1}$, $\kappa \in (0, \rho)$ and

$$\rho = -\lambda_{max}\left(P^{1/2}(A + B(K_0 + K))P^{-1/2} + P^{-1/2}(A + B(K_0 + K))^\top P^{1/2}\right) > 0,$$

then the origin of the closed-loop system (1) *with the homogeneous feedback law $u(t) = u_{hom}(x(t))$ given by* (25), *is globally uniformly finite-time stable and the settling time admits the estimate*

$$T(x_0) \leq \frac{\lambda_{\max}(P^{1/2}G_{\mathbf{d}}P^{-1/2} + P^{-1/2}G_{\mathbf{d}}^\top P^{1/2})\|x_0\|_{\mathbf{d}}}{2(\rho - \kappa)}. \tag{31}$$

The proof follows from the formula (9) that gives

$$\frac{d\|x\|_{\mathbf{d}}}{dt} = \|x\|_{\mathbf{d}}\frac{x^\top\mathbf{d}^\top(-\ln\|x\|_{\mathbf{d}})P\mathbf{d}(-\ln\|x\|_{\mathbf{d}})(Ax+Bu_{hom}(x)+f(t,x))}{x^\top\mathbf{d}^\top(-\ln\|x\|_{\mathbf{d}})PG_{\mathbf{d}}\mathbf{d}(-\ln\|x\|_{\mathbf{d}})x}.$$

Using the $\mathbf{d}$-homogeneity of the vector field $x \mapsto Ax + Bu_{hom}(x)$ and the estimate (30) yields

$$\frac{d\|x\|_{\mathbf{d}}}{dt} = \frac{x^\top\mathbf{d}^\top(-\ln\|x\|_{\mathbf{d}})P(A+BK_0+BK)\mathbf{d}(-\ln\|x\|_{\mathbf{d}})x + \|x\|_{\mathbf{d}}x^\top\mathbf{d}(-\ln\|x\|_{\mathbf{d}})P\mathbf{d}(-\ln\|x\|_{\mathbf{d}})f}{x^\top\mathbf{d}^\top(-\ln\|x\|_{\mathbf{d}})PG_{\mathbf{d}}\mathbf{d}(-\ln\|x\|_{\mathbf{d}})x}$$

$$\leq \frac{-\rho+\kappa}{x^\top\mathbf{d}^\top(-\ln\|x\|_{\mathbf{d}})PG_{\mathbf{d}}\mathbf{d}(-\ln\|x\|_{\mathbf{d}})x} \leq \frac{-2(\rho-\kappa)}{\lambda_{\max}(P^{1/2}G_{\mathbf{d}}P^{-1/2}+P^{-1/2}G_{\mathbf{d}}^\top P^{1/2})}.$$

Due to (28), (29) it follows that $\rho > 0$ and by construction $\rho - \kappa > 0$. Therefore, the canonical homogeneous norm is the Lyapunov function of the finite-time stable system (1), (25) with the settling time estimate (31). The settling time estimate (31) has minor conservatism due to system uncertainties. In the disturbance-free case, this estimate (inequality) may be exact (identity), see [18, page 302]. The considered homogeneous controller is a SMC algorithm with the sliding surface $x = 0$ and it has properties similar to the so-called quasi-continuous high order sliding mode controller [6]. Indeed, it is discontinuous only the sliding set $x = 0$, it steers all trajectories of the system to the sliding manifold $x = 0$ in a finite time and it rejects non-vanishing matched bounded perturbations.

Remark 2 *For $f(t,x) = Bq(t,x)$ the inequality*

$$\|P^{1/2}Bq(t,x)\| \le 0.5\kappa\lambda_{\min}(P^{1/2}G_{\mathbf{d}}P^{-1/2} + P^{-1/2}G_{\mathbf{d}}^{\top}P^{1/2})$$

implies (30)*. Indeed, from the identities* (26) (27)*, we conclude* $\mathbf{d}(-\ln\|x\|_{\mathbf{d}})B = \|x\|_{\mathbf{d}}^{-1}B$*, but the definition of the canonical homogeneous norm gives*

$$\|P^{1/2}\mathbf{d}(-\ln\|x\|_{\mathbf{d}})x\| = 1.$$

Hence, using the Schwarz inequality it is derived that

$$\|x\|_{\mathbf{d}}\|x^{\top}\mathbf{d}(-\ln\|x\|_{\mathbf{d}})P\mathbf{d}(-\ln\|x\|_{\mathbf{d}})f(t,x)\| \le \|P^{1/2}Bq(t,x)\| \le \kappa.$$

This means that the controller (25)*, indeed, rejects some non-vanishing bounded matched perturbations.*

Notice that, similarly to the unit SMC, the term

$$K_{hom}(\rho) := K_0 + \rho^{1+\mu}Ke^{-G_{\mathbf{d}}\ln\rho}, \quad \rho > 0 \tag{32}$$

in (25) can be treated as a state-dependent feedback gain of a linear controller, *i.e.*,

$$u_{hom} = K_{hom}(\|x\|_{\mathbf{d}})x, \qquad K_{hom} : (0,+\infty) \to \mathbb{R}^{m\times n}.$$

The choice $K = K_{lin} - K_0$ leads to $K_{hom}(1) = K_{lin}$, *i.e.*, the homogeneous controller coincides with the linear one on the unit sphere $x^{\top}Px = 1$. Notice that $\|x\|_P = 1 \Leftrightarrow \|x\|_{\mathbf{d}} = 1$. This feature is used for upgrading a linear feedback to a locally homogeneous SMC following the methodology introduced in [40]. Let us introduce the following saturation function:

$$sat_{\delta,\beta}(\varphi) = \begin{cases} \delta & \text{if} \quad \varphi < \delta, \\ \varphi & \text{if} \quad \delta \le \varphi \le \beta, \\ \beta & \text{if} \quad \varphi > \beta. \end{cases} \tag{33}$$

Theorem 4 *Let the matrix $K_{lin} \in \mathbb{R}^{m\times n}$ be the gain of a linear stabilizing feedback* (2)*, the pair $\{A,B\}$ be controllable, the matrices $G_{\mathbf{d}}$, K_0 be defined by the formulas* (27) (26) *and*

$$K \triangleq K_{lin} - K_0.$$

If $P \in \mathbb{R}^{n\times n}$ is a solution of the following LMI

$$\begin{cases} (A+BK_{lin})P + P^\top (A+BK_{lin}) \prec 0, \\ PG_{\mathbf{d}} + G_{\mathbf{d}}^\top P \succ 0, \quad P \succ 0, \end{cases} \tag{34}$$

and the function $f : \mathbb{R} \times \mathbb{R}^n \to \mathbb{R}^n$ satisfies (30) *for all x such that $\|x\|_P \le 1$ and*

$$2x^\top P f(t,x) \le \kappa x^\top P x, \quad \forall t > 0, \quad \forall x : \|x\|_P > 1, \tag{35}$$

where $\kappa \in [0, \rho)$ and $\rho > 0$ is defined in Proposition 1, then

- *the control law*

$$\tilde{u}(x) = K_{hom}(\mathrm{sat}_{0,1}(\|x\|_{\mathbf{d}}))x \tag{36}$$

  is continuous on $\mathbb{R}^n$ and it coincides with the linear feedback $u_{lin}(x)$ for $\|x\|_P \ge 1$ and with the homogeneous feedback $u_{hom}(x)$ for $\|x\|_P < 1$;

- *the origin of the closed-loop system* (1) (36) *is globally uniformly finite-time stable with the settling time estimate*

$$T(x_0) \le \begin{cases} \frac{1+2\ln(\|x_0\|)}{\rho-\kappa} + & \text{if} \quad \|x_0\|_P > 1, \\ \frac{\|x_0\|_{\mathbf{d}}}{\rho-\kappa} & \text{if} \quad \|x_0\|_P \le 1. \end{cases} \tag{37}$$

Proof. For $\|x_0\|_P \le 1$, the local finite-time stability of the closed-loop system follows from Proposition 1. For $\|x\|_P > 1$ we have $\tilde{u}(x) = K_{hom}(1)x = K_{lin}x$ and

$$\frac{d\|x\|_P}{dt} = \frac{x^\top\left((A+BK_{lin})P + P(A+BK_{lin})^\top\right)x + 2x^\top P f(t,x)}{2\|x\|_P} \le \frac{-\rho+\kappa}{2}\|x\|_P,$$

where the definition of the parameter ρ (see Proposition 1). This means that the function $V : \mathbb{R}^n \to \mathbb{R}$ given by

$$V(x) = \begin{cases} \|x\|_P & \text{if} \quad x^\top P x \ge 1 \\ \|x\|_{\mathbf{d}} & \text{if} \quad x^\top P x < 1, \end{cases}$$

is a Lyapunov function, and the closed-loop system is globally uniformly finite-time stable with the settling-time estimate (37). ■

According to the latter theorem, the existing linear controller can be transformed to a locally homogeneous SMC by means of a modification of the homogeneous scaling of the linear feedback gain close to the origin (see Fig. 2).

5 Digital Implementation of the Controllers

The control algorithms considered above deal with a continuous-time model of the system. In the case of a digital control device, the control input changes its value only at certain discrete instances of time:

$$0 = t_0 < t_1 < ... < t_k < \dots.$$

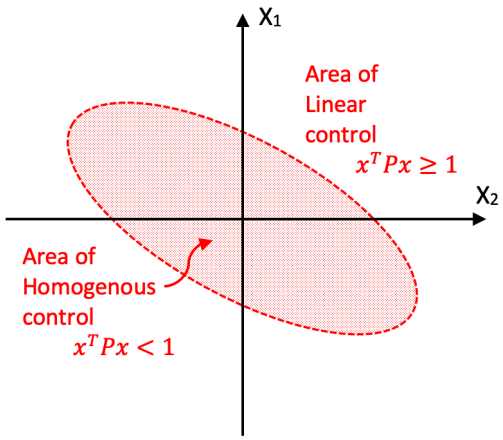

Figure 2: The illustration of the upgrade from linear to homogeneous controller.

The sampling period $h \triangleq t_{k+1} - t_k > 0$ can be constant (synchronous sampling) or time-varying (asynchronous sampling). Therefore, a more realistic model of the control system (1) with a digital controller is

$$\dot{x}(t) = Ax(t) + Bu(t_k), \quad \text{for } t \in [t_k, t_{k+1}). \tag{38}$$

In this case, the digital implementation of a continuous-time feedback control $u(\cdot)$ needs to be discretized somehow. Some classical schemes for discrete-time approximations of continuous-time systems can be used for this purpose. Let us recall that the explicit and implicit Euler methods are standard schemes for the discrete-time approximation of a nonlinear ODE:

$$\dot{x} = F(x), \quad F : \mathbb{R}^n \to \mathbb{R}^n.$$

Since for small $h > 0$ the approximation $\dot{x}(t) \approx \frac{x(t+h)-x(t)}{h}$ holds, then the approximate discrete-time models can be written as:

$$\tilde{x}_{k+1} = x_k + hF(x_k), \qquad \text{(explicit Euler method)}$$

and

$$\tilde{x}_{k+1} = x_k + hF(\tilde{x}_{k+1}), \qquad \text{(implicit Euler method)},$$

where $x_k = x(t_k)$ and $\tilde{x}_{k+1} \approx x(t_{k+1})$. If $F(\cdot)$ is a set-valued mapping, this defines a differential inclusion, and the analogous approximation of the time derivative leads to a discrete-time inclusion (see Section 5.2). For the linear plant (38) the following exact discrete-time approximation can be derived:

$$x_{k+1} = A_h x_k + B_h u(t_k) \tag{39}$$

where $x_k = x(t_k)$ and:

$$A_h = e^{hA} \text{ and } B_h = \int_0^h e^{A\tau} d\tau B. \tag{40}$$

The explicit Euler method presented above yields

$$A_h = I_n + hA \text{ and } B_h = hB. \tag{41}$$

For a small $h > 0$ the approximations $e^{Ah} \approx I_n + hA$ and $\int_0^h e^{A\tau} d\tau B \approx hB$ hold true. Following Euler's methods, the digital implementation of a feedback controller $u(x)$ for (38) given by

$$u(t_k) = u(x_k), \tag{42}$$

which is called an *explicit* discretization, and the scheme

$$u(t_k) = u(\tilde{x}_{k+1}) \tag{43}$$

is called an *implicit* discretization. In the latter case, in order to implement the controller in a digital device, the system of equations (39) and (43) has to be solved with respect to $\tilde{x}_{k+1}$, numerically and on-line. For feedback controllers allowing the representation

$$u(x) = \tilde{u}(x, x) \tag{44}$$

where the function $\tilde{u} : \mathbb{R}^n \times \mathbb{R}^n \to \mathbb{R}^m$ is linear in the second argument, the following *semi-implicit discretization* scheme given by

$$u(t_k) = \tilde{u}(x_k, x_{k+1}).$$

is also considered below. In [25] it is shown that the conventional explicit and implicit Euler schemes may produce in some cases a discrete-time model inconsistent with the original continuous-time system with respect to the stability properties (such as the convergence rate). For example, the finite-time stability of the homogeneous system with negative degree is always broken by Euler discretization. The so-called *consistent discretization* of the homogeneous systems is introduced in [25]. The proposed methodology is shown to be efficient for numerical simulation of closed-loop systems. In this paper, we compare the explicit, semi-implicit and implicit discretization of the controllers (2), (11) and (25) in the sense explained above.

Remark 3 *It is clear that the explicit and the implicit schemes yield controllers with different structures. This is a quite classical consequence of different discretization methods [41]. For instance, the explicit Euler discretization of the linear dynamics $\dot{x}(t) = Ax(t)$ yields $x_{k+1} = (I_n + hA)x_k$, while its implicit discretization yields $x_{k+1} = (I_n - hA)^{-1}x_k$. Such differences also appear in the context of feedback control as is visible in the next sections (in particular for the SMC).*

5.1 Discretizations of the Linear Controller

5.1.1 Explicit Scheme

The explicit discretization of the linear feedback leads to

$$u_k = K_{lin} x_k, \tag{45}$$

and the closed-loop discrete-time model has the form

$$x_{k+1} = (A_h + B_h K_{lin}) x_k.$$

Therefore, $A_h + B_h K_{lin}$ has to be a Schur matrix[3] to guarantee the exponential stability of the closed-loop system.

5.1.2 Semi-Implicit Scheme

Selecting

$$\tilde{u}(y, z) = \frac{1}{2} K_{lin} y + \frac{1}{2} K_{lin} z, \quad y, z, \in \mathbb{R}^n,$$

it follows that the linear feedback (2) possesses the form (43) and the semi-implicit discretization of the linear controller has the form

$$u_k = \frac{1}{2} K_{lin} x_k + \frac{1}{2} K_{lin} x_{k+1}.$$

Substituting $u(t_k)$ to (39) yields

$$(I_n - \frac{1}{2} B_h K_{lin}) x_{k+1} = (A_h + \frac{1}{2} B_h K_{lin}) x_k. \tag{46}$$

The matrix in the left-hand side of (46) is invertible for a sufficiently small $h > 0$, so

$$x_{k+1} = \left(I_n - \frac{1}{2} B_h K_{lin} \right)^{-1} \left(A_h + \frac{1}{2} B_h K_{lin} \right) x_k$$

and the semi-implicit discretization of the linear controller has the form

$$u_k = \frac{1}{2} K_{lin} \left(I_n + \left(I_n - \frac{1}{2} B_h K_{lin} \right)^{-1} \left(A_h + \frac{1}{2} B_h K_{lin} \right) \right) x_k. \tag{47}$$

Notice that $\left(I_n - \frac{1}{2} B_h K_{lin} \right)^{-1} \left(A_h + \frac{1}{2} B_h K_{lin} \right)$ has to be a Schur matrix to guarantee the exponential stability of the closed-loop system (39) (47).

[3] A matrix $Q \in \mathbb{R}^{n \times n}$ is said to be a Schur matrix if its spectral radius is less than 1.

5.1.3 Implicit Scheme

The implicit discretization of the linear feedback is

$$u_k = K_{lin} x_{k+1}.$$

In this case, it follows from (39) that

$$x_{k+1} = (I_n - B_h K_{lin})^{-1} A_h x_k.$$

Therefore, at each sampling instant the control input is defined as follows

$$u_k = K_{lin}(I_n - B_h K_{lin})^{-1} A_h x_k. \tag{48}$$

The exponential stability of the closed-loop system (39) (48) is guaranteed if $(I_n - B_h K_{lin})^{-1} A_h$ is a Schur matrix.

5.2 Discretization of the Unit SMC

5.2.1 Explicit Scheme

The classical idea for chattering reduction of SMC is to replace the sign multifunction by a piecewise-linear saturation function, and, next, to tune its width parameter [1]. This widely used engineering trick is known, however, to decrease the closed-loop accuracy since it destroys the sliding-mode phase. Moreover the tuning of the parameters (saturation width *vs.* sampling time) is not straightforward in general [22]. This is what is done below, taking into account the structure of the proposed SMC. As shown above the SMC (11) (18) can be interpreted as a linear feedback

$$u_{SM} = K_{SM}(\|Cx\|)x,$$

with the state-dependent gain $K_{SM}(\|Cx\|)$ given by (24), which tends to infinity as $\|Cx\| \to 0$. The infinite gain in the linear controller contributes to the so-called chattering phenomenon [1, 11]. The simplest approach to reduce the chattering is to bound the gain $K_{SM}(\|Cx\|)$ close to singularity points. To avoid the infinite gain in the explicit discretization of the SMC, we re-define it as follows

$$\tilde{u}(x) = K_{SM}(sat_{\delta,\beta}(\|Cx\|))x, \tag{49}$$

where $\beta > 0$ is defined in the formula (18) and $\delta \in (0, \beta)$ is a tuning parameter. Obviously, $\delta = 0$ corresponds to the original SMC, but for $\delta = \beta$ it follows that

$$K_{SM}(sat_{\beta,\beta}(\|Cx_k\|)) = K_{lin},$$

i.e., the proposed controller becomes the linear feedback in the limit case. Therefore, a linear controller can be upgraded to a SMC. To avoid the degradation of the control quality, the following procedure can be used:

1) design the parameters of the SMC using Theorem 3 for some $\beta > 0$;

2) implement the control law (49) in a digital device with $\delta = \beta$ (linear feedback);

3) decrease the parameter δ while the control quality is improving.

The control quality in the latter scheme can be estimated through numerical simulations or performing experiments on a setup. It may include various indexes, which correspond to control precision, energetic optimality, chattering effects, *etc.*

5.2.2 Semi-Implicit Scheme

Following the scheme suggested above, the semi-implicit discretization of the SMC is defined as follows:

$$u_k = K_{SM}(\mathrm{sat}_{\delta,\beta}(\|Cx_k\|))x_{k+1}.$$

Substituting it into (39) yields

$$(I_n - B_h K_{SM}(\mathrm{sat}_{\delta,\beta}(\|Cx_k\|))x_{k+1} = A_h x_k.$$

To guarantee the invertibility of $(I_n - B_h K_{SM}(\mathrm{sat}_{\delta,\beta}(\|Cx_k\|))$, the parameter $h > 0$ must be sufficiently small. The sufficient condition is $\|B_h K_{SM}(\mathrm{sat}_{\delta,\beta}(\rho)\| < 1$ for all $\rho \in [\alpha, \beta]$. This leads to:

$$u_k = K_{SM}(\mathrm{sat}_{\delta,\beta}(\|Cx_k\|))(I_n - B_h K_{SM}(\mathrm{sat}_{\delta,\beta}(\|Cx_k\|))^{-1} A_h x_k. \tag{50}$$

5.2.3 Implicit Scheme

For the implicit discretization of the SMC, the discrete-time model (39) is used together with the sliding surface (14) introduced above. With such a model, the nominal sliding dynamics becomes

$$Cx_{k+1}^{nom} = CA_h x_k^{nom} + CB_h u_k^{nom},$$

and the discrete-time invariance condition $Cx_{k+1}^{nom} = Cx_k^{nom}$ leads us to

$$u_k^{nom} = (CB_h)^{-1} C(I - A_h) x_k^{nom}.$$

Thus, it follows that

$$K_{nom} = (CB_h)^{-1} C(I - A_h). \tag{51}$$

As before, the discrete-time controller takes the form

$$u_k = K_{nom} x_k - u_k^{sv}. \tag{52}$$

We now proceed with the design of the term u_k^{sv}. Following [21] and [23], the implicit discretization of the sliding dynamics (13) is considered, that is:

$$\begin{cases} \sigma_{k+1} = \sigma_k - CB_h u_k^{sv} + C \displaystyle\int_0^h e^{A\tau} d\tau f_k, & \text{(53a)} \\ \mathbf{M}(\tilde{\sigma}_{k+1}) \triangleq u_k^{sv} \in -\gamma(\tilde{\sigma}_{k+1})\mathrm{Sgn}(\tilde{\sigma}_{k+1}), & \text{(53b)} \\ \tilde{\sigma}_{k+1} = \sigma_k - \alpha CB_h u_k^{sv}, & \text{(53c)} \end{cases}$$

where γ is as given in (18) above, $\tilde{\sigma}_k$ is a virtual variable which allows us to make an *approximate selection* of the set-valued map $\mathbf{M}$, and $\alpha > 0$ is a constant gain to be tuned. The expression of the implicit discretization in (53a)-(53c) has been already developed and validated in [23]. The set of equations in (53b) (53c) is a generalized equation with unknown $\tilde{\sigma}_{k+1}$, to be solved at each time-step. Let us show how its solution can be calculated explicitly.

Definition 3 *A set-valued map $\mathbf{N} : \mathbb{R}^n \rightrightarrows \mathbb{R}^n$ is monotone if for any $(\varphi_i, \theta_i) \in \mathrm{Grph}(\mathbf{N})$, $i \in \{1, 2\}$,*

$$(\varphi_1 - \varphi_2)^\top (\theta_1 - \theta_2) \geq 0. \tag{54}$$

In addition, $\mathbf{N}(\cdot)$ is maximal monotone if its graph is not strictly contained in the graph of any other monotone map.

Two single-valued and Lipschitz continuous maps are associated with a maximal monotone mapping $\mathbf{N}(\cdot)$, namely the resolvent and the Yosida approximation of $\mathbf{N}(\cdot)$ of degree $\rho > 0$, which are defined respectively as

$$\mathcal{R}^\rho_{\mathbf{N}}(\varphi) = (I + \rho \mathbf{N})^{-1}(\varphi), \tag{55}$$

$$\mathcal{Y}^\rho_{\mathbf{N}}(\varphi) = \frac{1}{\rho} \left(I - \mathcal{R}^\rho_{\mathbf{N}}\right)(\varphi). \tag{56}$$

Roughly speaking, the Yosida approximation associated with $\mathbf{N}(\cdot)$ is an approximate minimal-norm selection of $\mathbf{N}(\cdot)$, in the sense that

$$\mathcal{Y}^\rho_{\mathbf{N}}(\varphi) \in \mathbf{N}\left(\mathcal{R}^\rho_{\mathbf{N}}(\varphi)\right),$$

with the particular property that $\mathcal{Y}^\rho_{\mathbf{N}}(\varphi) \to \arg\min_{\theta \in \mathbf{N}(\varphi)} |\theta|$ as $\rho \downarrow 0$, whereas the resolvent satisfies $\mathcal{R}^\rho_{\mathbf{N}}(\varphi) \to \varphi$ as $\rho \downarrow 0$, see, *e.g.*, [42]. For the scalar case, regarding the set-valued map $\mathbf{M}(\cdot)$ in (53b), it is indeed maximal monotone as proved now.

Proposition 2 *The set-valued map $\mathbf{M} : \mathbb{R} \rightrightarrows \mathbb{R}$ in* (53b) *is maximal monotone.*

Proof. It is clear that:

$$\mathbf{M}(v) = \begin{cases} -\lambda\varphi, & \text{if } \beta < |\varphi| \\ -\lambda\beta \mathrm{sgn}(\varphi), & \text{if } 0 < |\varphi| < \beta \\ [\lambda\beta, -\lambda\beta], & \text{if } \varphi = 0 \end{cases}, \tag{57}$$

where $\mathrm{sgn} : \mathbb{R} \setminus \{0\} \to \{-1, 1\}$ is the classical signum map so that $\varphi \mapsto -1$ if $\varphi < 0$, and $\varphi \mapsto 1$ if $\varphi > 0$. Notice that sgn is undefined at $\varphi = 0$. A simple, although lengthy, case by case analysis shows that (54) holds everywhere, whereas maximality follows from the outer semicontinuity of $\mathbf{M}$. Fig. 3 shows the graph of $\mathbf{M}$, confirming the maximal monotonicity of the operator. ■

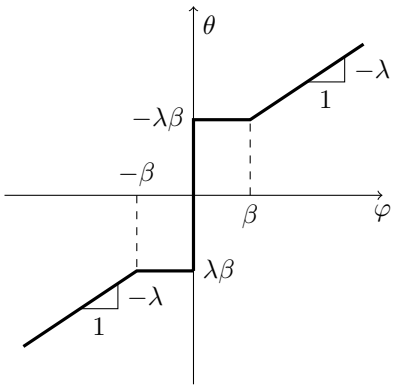

Figure 3: Graph of the set-valued map $\mathbf{M}(\cdot)$ defined in (53b) showing the local scope of the SMC and confirming the global maximal monotonicity of the map.

The maximal monotonicity of $\mathbf{M}(\cdot)$ guarantees that the generalized equation (GE) (53b)-(53c) has a unique solution. Indeed, the substitution of (53b) into (53c) yields the GE

$$\tilde{\sigma}_{k+1} \in \sigma_k + \rho_h \gamma(\tilde{\sigma}_{k+1}) \mathrm{Sgn}(\tilde{\sigma}_{k+1}) = \sigma_k - \rho_h \mathbf{M}(\tilde{\sigma}_{k+1}),$$

where $\rho_h = \alpha C B_h > 0$, which in view of (55) has the solution

$$\tilde{\sigma}_{k+1} = \mathcal{R}_{\mathbf{M}}^{\rho_h}(\sigma_k). \tag{58}$$

The substitution of (58) back into (53c) yields:

$$u_k^{sv} = \frac{1}{\rho_h} \left(\sigma_k - \mathcal{R}_{\mathbf{M}}^{\rho_h}(\sigma_k) \right) = \mathcal{Y}_{\mathbf{M}}^{\rho_h}(\sigma_k). \tag{59}$$

It is possible to provide an explicit expression for both, the resolvent and the Yosida approximation. Indeed, setting $\delta_h = -\rho_h \lambda \beta$, a case by case analysis of (57) yields

$$\mathcal{R}_{\mathbf{M}}^{\rho_h}(\sigma_k) = \begin{cases} \frac{1}{1-\rho_h \lambda} \sigma_k, & \text{if } \beta + \delta_h \leq |\sigma_k| \\ \sigma_k + \rho_h \lambda \beta \mathrm{sgn}(\sigma_k), & \text{if } \delta_h < |\sigma_k| < \beta + \delta_h \\ 0, & \text{if } |\sigma_k| \leq \delta_h \end{cases}, \tag{60}$$

$$\mathcal{Y}_{\mathbf{M}}^{\rho_h}(\sigma_k) = \begin{cases} \frac{-\lambda}{1-\rho_h \lambda} \sigma_k, & \text{if } \beta + \delta_h \leq |\sigma_k| \\ -\lambda \beta \mathrm{sgn}(\sigma_k), & \text{if } \delta_h < |\sigma_k| < \beta + \delta_h \\ \frac{1}{\rho_h} \sigma_k, & \text{if } |\sigma_k| \leq \delta_h \end{cases}. \tag{61}$$

Note that both $\rho_h = o(h)$ and $\delta_h = o(h)$, where $o(h)$ denotes the classical "little o" notation, that is $\lim_{h \to 0} \frac{o(h)}{h} = 0$. Thus, a study similar to the one done in [23, Section 4.5] shows that the trajectories of the discrete-time closed-loop system converge to trajectories of the continuous-time closed-loop as $h \downarrow 0$. *It is inferred that the generalized equation in (53b) (53c) has a solution which can be easily computed online at each timestep.*

5.3 Discretization of the Homogeneous SMC

5.3.1 Explicit Scheme

Since the gain (32) of the homogeneous control tends to infinity as $\|x\| \to 0$, the saturation function $\mathrm{sat}_{\alpha,\beta}$ is used to regularize this singularity similarly to the unit SMC considered above:

$$u(t_k) = K_{hom}(\mathrm{sat}_{\delta,1}\|x_k\|_{\mathbf{d}})x_k, \tag{62}$$

where $0 < \delta \leq 1$ are tuning parameters. For $\delta = 1$, we have $K_{hom}(\mathrm{sat}_{1,1}\|x_k\|_{\mathbf{d}}) = K_{lin}$, the proposed controller coincides with the linear controller. Therefore, a linear controller can be upgraded to homogeneous SMC while avoiding any degradation of the control precision using the following procedure [40]:

1) design the parameters of the homogeneous controller using Theorem 4;

2) implement the control law (62) in a digital device with $\delta = 1$ (linear feedback);

3) decrease the parameter $\delta \in (0, 1)$ while the control quality is improving.

Notice that $K_{hom}(\mathrm{sat}_{\delta,1}\|x\|_{\mathbf{d}}) = K_{lin}$ for $\|x\| \geq 1$, *i.e.*, in this case, the homogeneous controller modifies the linear feedback only locally (close to 0). In the latter case, the exponential stability of the system (39) (45) implies at least the practical asymptotic stability (convergence to a bounded zone) for the closed-loop system (39) (62). An additional difficulty for the application of the homogeneous controller is the computation of the canonical homogeneous norm defined implicitly (see the formula (8)). Fortunately, a rather simple procedure can be used for the on-line computation of the canonical homogeneous norm (see, *e.g.*, [40]).

5.3.2 Semi-Implicit Scheme

The semi-implicit discretization of the homogeneous control gives

$$u(t_k) = K_{hom}(\mathrm{sat}_{\delta,1}\|x_k\|_{\mathbf{d}})x_{k+1}.$$

Using (39) yields

$$(I_n - B_h K_{hom}(\mathrm{sat}_{\delta,1}\|x_k\|_{\mathbf{d}}))x_{k+1} = A_h x_k.$$

The matrix $I_n - B_h K_{hom}(1)$ is invertible for a sufficiently small $h > 0$. Then the matrix $I_n - B_h K_{hom}(\mathrm{sat}_{\delta,1}\|x_k\|_{\mathbf{d}})$ is invertible for some $0 < \delta < 1$, so it is inferred that

$$u(t_k) = K_{hom}(\mathrm{sat}_{\delta,1}\|x_k\|_{\mathbf{d}})(I_n - B_h K_{hom}(\mathrm{sat}_{\delta,1}\|x_k\|_{\mathbf{d}}))^{-1} A_h x_k. \tag{63}$$

Similarly to the case of the explicit discretization, the exponential stability of the system (39) (47) implies at least the practical asymptotic stability (convergence of solutions to a bounded zone) for the closed-loop system (39) (63).

5.3.3 Implicit Scheme

The so-called consistent discretization of the closed-loop system (1) (25) is studied in [25], where it was assumed that $P = P^\top \succ 0$ is selected such that

$$\begin{cases} (A + BK_0 + BK)^\top P + P(A + BK_0 + BK) + \rho(PG_{\mathbf{d}} + G_{\mathbf{d}}^\top P) = \mathbf{0}, \\ PG_{\mathbf{d}} + G_{\mathbf{d}}^\top P \succ 0, \end{cases} \tag{64}$$

where $\rho > 0$ is a tuning parameter. In this case, it follows that (see the proof of Proposition 1)

$$\frac{d}{dt}\|x\|_{\mathbf{d}} = -\rho.$$

Hence, for any trajectory of the closed-loop system (1) (25), it follows that $\|x(t_{k+1})\|_{\mathbf{d}} = \|x(t_k)\|_{\mathbf{d}} - \rho(t_{k+1} - t_k)$. Taking into account this theoretically exact estimate of $\|x(t_{k+1})\|_{\mathbf{d}}$ for the closed-loop continuous-time system, an implicit discretization of the controller (36) can be defined as

$$u(t_k) = K_{hom}(\mathrm{sat}_{\delta,1}(\|x_k\|_{\mathbf{d}} - \rho h)x_{k+1}$$

or, equivalently,

$$u(t_k) = K_{hom}(\mathrm{sat}_{\delta,1}(\|x_k\|_{\mathbf{d}} - \rho h))(I_n - B_h K_{hom}(\mathrm{sat}_{\delta,1}(\|x_k\|_{\mathbf{d}} - \rho h)))A_h x_k, \tag{65}$$

where $0 < \delta < 1$ is, as above, a tuning parameter, and the canonical homogeneous norm is induced by the norm $\|x\|_P = \sqrt{x^\top P x}$ with $P \succ 0$ being a solution of the following semi-definite programming problem:

$$\eta \to \min \tag{66}$$

subject to

$$\begin{cases} -\eta I_n \preceq (A + BK_{lin})^\top P + P(A + BK_{lin}) + \rho(PG_{\mathbf{d}} + G_{\mathbf{d}}^\top P) \preceq 0, \\ PG_{\mathbf{d}} + G_{\mathbf{d}}^\top P \succ 0, \quad P \succ 0, \quad 0 \le \eta \in \mathbb{R}. \end{cases} \tag{67}$$

Obviously, if the optimal η is zero, then (64) is fulfilled. Notice that the control (65) is just a possible implicit discretization of the continuous-time homogeneous feedback law inspired by [25].

6 Experimental Validation

The platform QUBE—Servo 2 of Quanser is used for the experiment. It is depicted in Fig. 4.

6.1 Rotary pendulum model

The parameters of the experimental platform are given by the manufacturer and they are listed in the Table 1. The rotary pendulum model is shown in Fig. 5. The rotary arm pivot is attached to the QUBE-Servo 2 system and

Figure 4: Rotary inverted pendulum.

is actuated. The arm has a length r, a moment of inertia J_r, and its angle θ increases positively when it rotates counter-clockwise (CCW). The servo (and thus the arm) should turn in the CCW direction when the control voltage is positive, $v_m > 0$. The pendulum link is connected to the end of the rotary arm. It has a total length of L_p and its center of mass is at $l = L_p/2$. The moment of inertia about its center of mass is J_p. The rotary pendulum angle α is zero when it is hanging downward and increases positively when rotated CCW. The equations of motion for the pendulum system are developed using

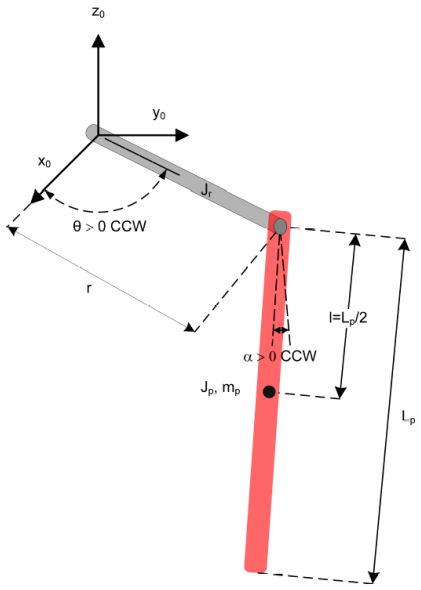

Figure 5: Rotary pendulum model.

the Euler-Lagrange method, from the total kinetic and potential energies of the

Table 1: Parameters of the pendulum QUBE—Servo 2

Parameter	Value
m_p	0.024 Kg
L_p	0.129 m
J_p	3.3×10^{-5} Kg.m^2
b_p	0.0015 N.m.s/rad
r	0.085 m
J_r	5.7×10^{-5}Kg.m^2
b_r	0.0005 N.m.s/rad
g	9.81 m/s^2

system. The nonlinear Lagrange dynamics is given as:

$$\begin{cases} \left(J_r + J_p \sin\alpha^2\right)\ddot{\theta} + m_p lr\cos\alpha\ddot{\alpha} + 2J_p \sin\alpha\cos\alpha\dot{\theta}\dot{\alpha} - m_p lr\sin\alpha\dot{\alpha}^2 = \tau - b_r\dot{\theta} \\ J_p\ddot{\alpha} + m_p lr\cos\alpha\ddot{\theta} - J_p\sin\alpha\cos\alpha\dot{\theta}^2 + m_p gl\sin\alpha = -b_p\dot{\alpha}, \end{cases} \tag{68}$$

where $J_r = m_r r^2/3$ is the moment of inertia of the rotary arm with respect to the pivot (*i.e.*, rotary arm axis of rotation) and $J_p = m_p L_p^2/3$ is the moment of inertia of the pendulum link relative to the pendulum pivot (*i.e.*, axis of rotation of pendulum). The viscous damping torques acting on the rotary arm and the pendulum link are b_r and b_p, respectively. The applied torque at the base of the rotary arm generated by the servo motor is

$$\tau = \frac{k_m}{R_m}\left(v_m - k_m\dot{\theta}\right).$$

6.2 Linear State-Space Model

When the nonlinear Lagrange dynamics is linearized around the operating point, the resulting linear dynamics for the rotary pendulum is given by

$$\begin{aligned} J_r\ddot{\theta} + m_p lr\ddot{\alpha} &= \tau - b_r\dot{\theta}, \\ J_p\ddot{\alpha} + m_p lr\ddot{\theta} + m_p gl\alpha &= -b_p\dot{\alpha}. \end{aligned}$$

Solving for the acceleration terms yields:

$$\begin{aligned} \ddot{\theta} &= \frac{1}{J_t}\left(m_p^2 l^2 rg\alpha - J_p b_r\dot{\theta} + m_p lrb_p\dot{\alpha} + J_p\tau\right), \\ \ddot{\alpha} &= \frac{1}{J_t}\left(-m_p glJ_r\alpha + m_p lrb_r\dot{\theta} - J_p b_p\dot{\alpha} - m_p rl\tau\right), \end{aligned}$$

where

$$J_t = J_p J_r - m_p^2 l^2 r^2.$$

The linear model of the pendulum system can be expressed in state-space form as

$$\dot{x}(t) = Ax(t) + Bv_m(t), \tag{69}$$

where $x(t) = \left[\theta(t), \alpha(t), \dot{\theta}(t), \dot{\alpha}(t)\right]^\top \in \mathbb{R}^4$ is the state vector, $v_m(t) \in \mathbb{R}$ is the control signal, $y(t) = [\theta(t)\ \ \alpha(t)]^\top$ is the output that is measured directly, $A \in \mathbb{R}^{4\times4}, B \in \mathbb{R}^{4\times1}$. Simplifying the dynamics by choosing $b_p = b_r = 0$, the matrices of the linear systems are

$$A = \begin{pmatrix} 0 & 0 & 1 & 0 \\ 0 & 0 & 0 & 1 \\ 0 & 149.2751 & -0.0104 & 0 \\ 0 & 261.6091 & -0.0103 & 0 \end{pmatrix},\ B = \begin{pmatrix} 0 \\ 0 \\ 49.7275 \\ 49.1493 \end{pmatrix}. \tag{70}$$

Since $\text{rank}(A) < 4$, the matrix A is not invertible. In order to find A_h, B_h of the discrete-time model (39), the Jordan decomposition $A = S^{-1}JS$ is adopted, where $J,\ S \in \mathbb{R}^{4\times4}$. Let J be the Jordan block diagonal $J = \text{diag}(0, J_1)$, where J_1 is a diagonal invertible matrix. Then $e^{J\tau} = \text{diag}(e^{0\tau}, e^{J_1\tau})$ and $\int_0^h e^{J\tau}d\tau = \int_0^h \text{diag}(e^{0\tau}, e^{J_1\tau})d\tau = \text{diag}(h, J_1^{-1}(e^{J_1h} - I))$. Then the implementation is given by

$$A_h = S^{-1}\,\text{diag}\left(1,\, e^{J_1h}\right)S, \tag{71}$$

$$B_h = S^{-1}\,\text{diag}\left(h, J_1^{-1}\left(e^{J_1h} - I_3\right)\right)SB, \tag{72}$$

where $I_3 \in \mathbb{R}^{3\times3}$ is the identity matrix.

6.3 Comparisons between the Controllers

The platform is supported with both a swing-up controller and a linear stabilizing controller realized in MATLAB. In this work only the linear stabilizing controller is modified. The conceptual scheme of the whole controller's architecture is depicted in Fig. 6. The switching from the energy swing-up to the stabilizing controllers occurs when the pendulum arm is in the upper position and remains in the bound $|\alpha| < 20$ deg, which takes approximately 3 sec. The experiments are carried out with a fixed sampling time $h > 0$, which is given by the encoder of the device for a total experimental time of 20 sec. The derivatives are not available directly from the output $y = [\theta\ \ \alpha]^\top$, so the linear differentiator $F(s) = 50s/(s+50)$ is used for getting the corresponding angular velocities. The gains of the linear proportional controllers are given by the manufacturer:

$$K_{lin} = \begin{bmatrix} 2 & -35 & 1.5 & -3 \end{bmatrix}. \tag{73}$$

Thus, the matrix $A + BK_{lin}$ has the following eigenvalues

$$\lambda_1 = -48.2522;\ \lambda_2 = -11.4050 + 0.4427i;$$
$$\lambda_3 = -11.4050 - 0.4427i;\ \lambda_4 = -1.8048.$$

Two eigenvalues are real negative and can be used for the upgrade since Assumption 1 is fulfilled for both. The experiments showed that the choice of $\Lambda = \lambda_4$ produces a better precision in θ trajectory tracking with less control effort. For

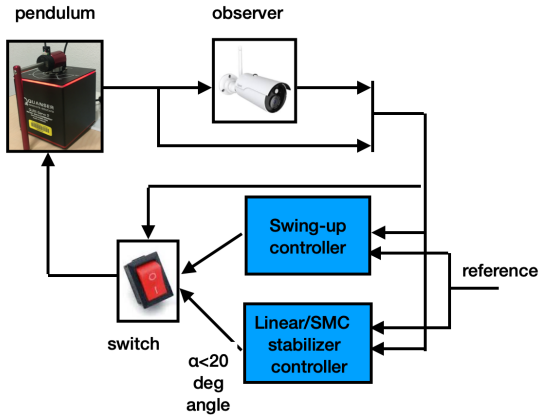

Figure 6: Conceptual scheme of the controller for the rotary inverted pendulum.

this reason, in the subsequent study, $\Lambda = \lambda_4$ is used for the computation of the unit SMC.

$$C = \begin{bmatrix} -1.1081 & 2.5670 & -0.2170 & 0.2399 \end{bmatrix};$$
$$K_{nom} = \begin{bmatrix} 0 & -30.3668 & 1.1084 & -2.5670 \end{bmatrix}.$$

The parameters of the homogeneous controller are obtained using the optimization procedure (66) with $\rho = 0.3$ and the formulas (26) (27):

$$G_{\mathbf{d}} = \begin{bmatrix} 4 & -2.0235 & 0 & 0 \\ 0 & 2 & 0 & 0 \\ 0 & 0 & 3 & -2.0235 \\ 0 & 0 & 0 & 1 \end{bmatrix}$$

$$P = \begin{bmatrix} 0.384292104901 & -0.359309495138 & -0.461690196545 & 0.249679449507 \\ 0.004218404736 & 0.007818126479 & 0.015300458661 & -0.109573955271 \\ -0.507371655307 & 0.480799179592 & 1.634211664648 & 2.794710688710 \\ -0.029849820347 & -0.063892496508 & 0.355937378044 & 2.595604268900 \end{bmatrix}$$

$$K_0 = \begin{bmatrix} 0 & -5.3227425 & 0.042 & 0 \end{bmatrix}.$$

In practice, in order to simplify the computation of the gain K_{hom}, the Jordan transformation of the matrix $G_{\mathbf{d}}$ can be used. The aim of the controller is to stabilize the pendulum arm (the angle α) at the upper unstable position and to minimize the tracking error between θ (the angle of the rotary arm) and a reference signal θ_{ref}. Three scenarios are tested:

1) Regulation: $\theta_{ref} = 0$ rad;

2) Sinusoidal reference: $\theta_{ref}(t) = 0.3sin(t)$ rad;

3) Step reference: $\theta_{ref}(t) = \begin{cases} 0 \text{ rad} & \text{if} \quad t \in [0, 5) \text{ s.} \\ 0.6 \text{ rad} & \text{if} \quad t \in [5, 10) \text{ s.} \\ -0.6 \text{ rad} & \text{if} \quad t \in [10, 15) \text{ s.} \\ 0 \text{ rad} & \text{if} \quad t \in [15, 20] \text{ s.} \end{cases}$.

In all the experiments, the swing-up controller is active during approximately 3 s. Thus, a comparison of the algorithms' performances is made using the L^2 and L^∞ norms of both the input u and the tracking error $e_\theta = \theta - \theta_{ref}$ on the time interval $[3, 20]$ s. The average of three tests is considered for each result given below, to take into account the uncertainty of $\theta \pm 0.02$ rad.

6.3.1 Regulation

Figure 7 shows the time-trajectories for the explicit, the semi-implicit, and the implicit discretization of the three control strategies of Section 5. In each experiment, the nominal sampling time $h = 0.002$ sec. was used, together with the control parameters $\delta = 0.65$, $\beta = 1$ for the explicit and semi-implicit SMC; $\rho_h = 50$, $\beta = 1$ for implicit SMC; and $\delta = 0.75$, $\beta = 1$ for the homogeneous controller. It can be appreciated that the regulated variable θ reaches a neighborhood of the reference $\theta_{ref} = 0$ in approximately 4 sec. In the implicit case, it is notable that the SMC is the only strategy presenting a very smooth stabilization after approximately 12 sec with a constant error in θ of approximately 0.02 rad. Additionally, chattering is successfully counteracted. This confirms once again previous results [22, 27, 28] obtained on different systems (an electropneumatic system and an inverted pendulum on a cart).

6.3.2 Tracking

Although the original design was made for regulation, in this section the performance and robustness (against uncertainty in the exact sampling time) of the controllers was put into test in the more general setting of signal tracking. Tables 2 and 3 show the performance of the three controllers for two different reference signals. For each case, the nominal sampling time $h = 0.002$ sec is set first. Afterwards, the experiment is repeated without changing the controller parameters but with a sampling time $h = 0.008$ sec. In all cases, the performance is evaluated using the L^2 and the L^∞ norms of the tracking error for the angle θ and the control input u during the stabilization stage, *i.e.*, the norms are taken on the time interval $[3, 20]$. In addition, following [22, 27, 28], the nearest integer approximation of the total variation of the control input (denoted as $\lfloor \text{Var}(u) \rceil$), is computed as an estimate of the quality of the input signal. For a discrete-time signal u, the total variation during the interval $[t_k, t_N]$ is given by

$$\text{Var}(u) \triangleq \sum_{i=k}^{N} |u_{i+1} - u_i|.$$

Thereby, control inputs with high variation undergo either chattering, or large overshoots/undershoots, or both. For the cases where there are neither over-

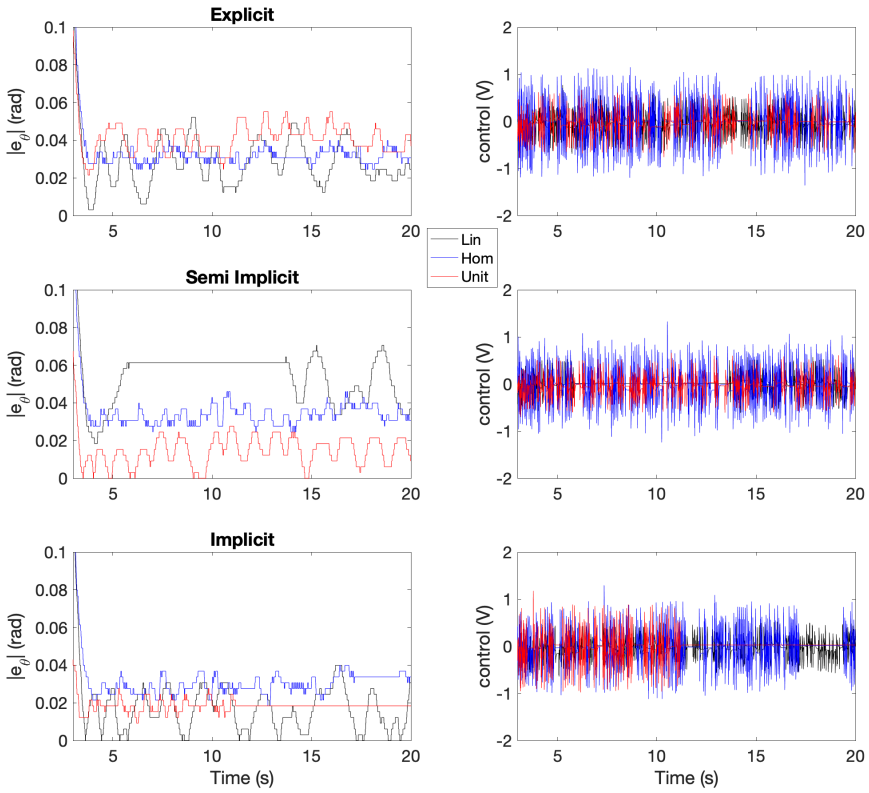

Figure 7: Comparison of the controllers in explicit, semi-implicit, and implicit for $h = 0.002$ in the case of stabilization at $\theta_{ref} = 0$.

shoots nor undershoots, the variation of the control signal is a reasonable quantifier of the chattering in the controller. The control parameters remain as before, that is $\delta = 0.65$, $\beta = 1$ for the explicit and semi-implicit SMC; $\rho_h = 50$, $\beta = 1$ for implicit SMC; and $\delta = 0.75$, $\beta = 1$ for the homogeneous controller. During the parameter-tuning process made in the tracking sinusoidal case, experiments (not explained in detail here) showed that the smaller δ, the smaller the tracking error in θ, but with more accentuated control effort, and *vice-versa*. Therefore, the additional parameter δ must be carefully tuned, depending on the constraints of the application. Figures 8 and 9 depict the transients of the trajectory tracking and control signal in sinusoidal and step cases. To explain the tables we can proceed in vertical or horizontal reading. In the first vertical reading case we compare the explicit, implicit and semi-implicit discretizations for the three controllers. As the reference point for the comparison we take the

Table 2: Case 1: Sinusoidal reference

	$h = 0.002$					$h = 0.008$				
	$\|e_\theta\|_{L^2}$	$\|u\|_{L^2}$	$\|e_\theta\|_{L^\infty}$	$\|u\|_{L^\infty}$	$\lfloor \mathrm{Var}(u) \rceil$	$\|e_\theta\|_{L^2}$	$\|u\|_{L^2}$	$\|e_\theta\|_{L^\infty}$	$\|u\|_{L^\infty}$	$\lfloor \mathrm{Var}(u) \rceil$
Explicit										
Lin	0.327	1.163	0.132	0.984	606	0.367	1.213	0.147	0.967	362
Unit	0.249	1.219	0.108	1.033	703	0.256	1.273	0.120	0.956	415
Hom	0.174	1.968	0.077	1.573	1489	0.239	2.630	0.106	1.804	891
Semi Implicit										
Lin	0.266	1.166	0.113	0.989	576	0.359	1.184	0.150	1.033	340
Unit	0.189	1.124	0.087	0.926	586	0.258	1.216	0.115	0.919	358
Hom	0.222	1.667	0.106	1.328	1200	0.227	1.952	0.200	1.557	702
Implicit										
Lin	—	—	—	—	—	—	—	—	—	—
Unit	0.135	1.589	0.060	1.408	1239	0.141	1.914	0.067	1.543	708
Hom	0.169	1.650	0.078	1.278	1207	0.637	3.980	0.342	4.290	7350

Table 3: Case 2: Step reference

	$h = 0.002$					$h = 0.008$				
	$\|e_\theta\|_{L^2}$	$\|u\|_{L^2}$	$\|e_\theta\|_{L^\infty}$	$\|u\|_{L^\infty}$	$\lfloor \mathrm{Var}(u) \rceil$	$\|e_\theta\|_{L^2}$	$\|u\|_{L^2}$	$\|e_\theta\|_{L^\infty}$	$\|u\|_{L^\infty}$	$\lfloor \mathrm{Var}(u) \rceil$
Explicit										
Lin	1.020	1.481	1.211	2.911	479	1.021	1.522	1.214	2.753	291
Unit	0.957	1.623	1.241	3.288	520	0.926	1.703	1.214	2.587	327
Hom	0.963	2.277	1.229	6.290	980	0.962	3.137	1.238	5.420	839
Semi Implicit										
Lin	1.023	1.422	1.226	2.668	424	0.979	1.537	1.183	2.781	268
Unit	0.954	1.570	1.241	2.811	459	0.951	1.643	1.263	2.502	300
Hom	0.964	2.029	1.235	5.366	809	0.973	2.296	1.248	4.906	628
Implicit										
Lin	1.023	1.436	1.229	2.566	444	1.023	1.508	1.248	2.975	258
Unit	0.897	1.933	1.260	2.899	763	0.895	2.237	1.269	3.140	585
Hom	0.964	1.987	1.232	5.067	765	1.032	4.080	1.174	5.120	7054

explicitly discretized linear controller (provided by the manufacturer).

Fig. 7 shows a comparison between the three controllers in the nominal condition and in the stabilization case. The given linear controller is already well tuned by the manufacturer specifically for the stabilization of the rotary inverted pendulum, so the improvement cannot be high in this case. Figure 7 is mainly aimed to confirm that there is no degradation of control quality after the upgrade. However, there is a minor improvement even in this case provided that nonlinear algorithms are properly discretized. Figures 8 and 9 show a more evident performance's improvement.

Some general conclusions about the experiments:

- The linear controller has always the worst trajectory tracking performance. In some scenarios an improvement of the tracking precision by nonlinear controllers is larger than 40%.

- The unit and homogeneous SMCs achieve comparable results in term of trajectory tracking, but the unit SMC presents less control effort. This

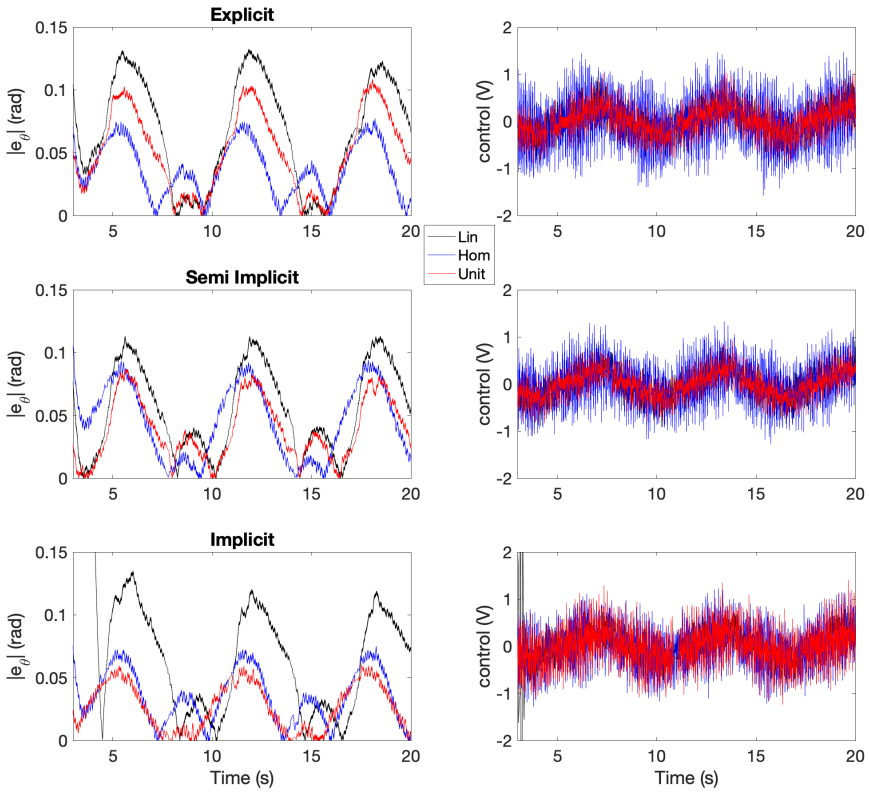

Figure 8: Comparison of the controllers in explicit, semi-implicit, and implicit for $h = 0.002$ in the case of sinusoidal reference.

means that the chattering is effectively reduced. This is probably caused by the nature of the homogeneous feedback which scales "dynamically" (depending on the homogeneous norm of the tracking error) *all eigenvalues* of the closed-loop error system, while the unit SMC deals only with one (closest to zero) eigenvalue.

- It is clear that the implicit discretization of the unit SMC can allow the best trajectory tracking and robustness with respect to the sampling time variation, while keeping an acceptable control effort.

- The semi-implicitly discretized unit SMC improves the tracking precision (up to 40% in some scenarios) *without degradation of the input signal quality.*

A detailed analysis of the results: The implicit discretization in the sinu-

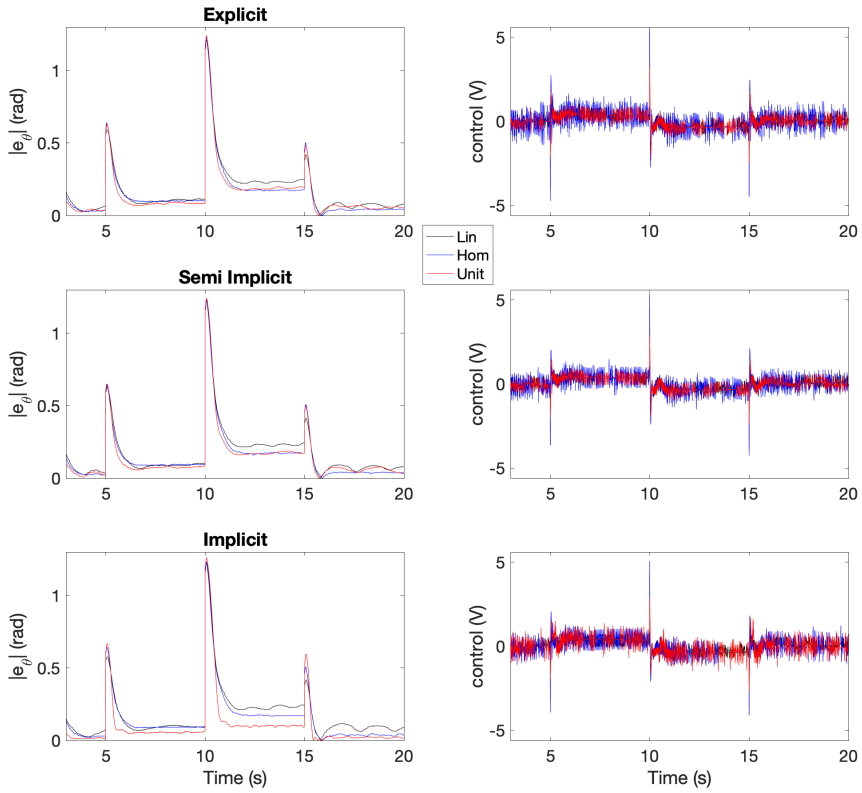

Figure 9: Comparison of the controllers in explicit, semi-implicit, and implicit for $h = 0.002$ in the case of step reference.

soidal case does not allow the linear controller to stabilize the tracking error in less than 3 sec. In the sinusoidal reference trajectory case and explicit discretization, the homogeneous controller (which has the best precision) has an accuracy improvement of 46% with respect to the linear one, but with an increase of 69% in control energy. The implicit SMC has an improvement of 45% with respect to the explicit SMC, but with an increase of 30% in control energy. In the step reference case and explicit discretization, the SMC (which has the best performance) has an improvement of 6% with respect to the linear one but with an increase of 9.5% in control energy, the implicit SMC (which has the best precision) has an improvement of 6% with respect to the explicit SMC, but with an increase of 19% in the control energy.

The robustness of the controllers with respect to the sampling time variation ($h = 0.008$) is also checked. This can happen in some control systems in case

of data-loss, or of a modification of the characteristics of internal electronics components (caused by heating, cooling down, or wear). Past experimental works on SMC [22, 28, 27] have proved that the implicit method bears for large sampling times without deteriorating too much the closed-loop performance. It is clear that in both step and sinusoidal scenarios, the trajectory tracking and the control effort in linear and SMCs are comparable to the nominal sampling time ($h = 0.002$), meaning that they are robust. But, the implicit homogeneous controller presents a degradation in the sinusoidal (resp. step) scenario of 276% (resp. 7%) in trajectory tracking, and of 141% (resp. 105%) in control quality. *This means that the sampling parameter h influences a lot the performance of the homogeneous controller in the case of the implicit discretization.* A development of a more robust implicit discretization scheme for homogeneous controllers is an interesting problem for the future research.

Finally it is noticeable in both Tables 2 and 3, that the implicit discretisation of the unit SM controller, does not decreases its total variation (which measures the chattering) compared with the explicit and the semi-implicit methods. This seems to be in contradiction with previous conclusions [22, 27, 28]. It seems, this is due to the fact that the transient period before the sliding surface is reached, is approximately equal to 12s, see the implicit scheme in Fig. 7. This is too long in case of the step reference (whose values switch from a constant value to another constant value after 5s). Hence the problem encountered in this case is that the SMC in this paper is designed for regulation, not for tracking. If the trajectory to be tracked is too fast, then the control design has to be changed in order to recover the chattering drastic reduction that is observed in the above stabilization experiments and and in the above cited articles with the implicit discretization. It is also noteworthy that the advantages that are brought by the implicit discretization, are visible only during the sliding phase. Indeed, during the reaching phase both the explicit and the implicit are known to behave equivalently, a fact confirmed by the data in Fig. 7.

7 Conclusion

In this article, a procedure to upgrade the linear controller to the unit sliding-mode controller (SMC) and to a homogeneous SMC is introduced. It modifies the linear feedback in a certain zone of the state space and transforms it to a SMC. Based on the structure of the obtained improved controllers, two special schemes of their practical implementation in semi-implicit and implicit discretizations are proposed. To make the mentioned upgrade, just two additional parameters needs to be tuned in practice. The tuning rules for these parameters prevent any degradation of the control quality. The theoretical results are supported by experiments performed on an inverted rotary pendulum, which is a nonlinear system. In practice the system performance is usually sacrificed due to the trade-off between the minimization of the chattering and the convergence performance. But this is not the case in this study, because a linear controller is transformed to a SMC. The proposed method incorporates tuning

rules to deal with this problem for the passage from the linear controller to the SMC. The obtained experimental results show that the upgrading strategies improve the tracking performance of the linear controller provided by the manufacturer, while keeping similar control signal in the sense of magnitude, energy and chattering index. The simplicity of the suggested scheme should allow many operating control systems to be upgraded easily.

References

[1] V. I. Utkin, *Sliding Modes in Control Optimization*. Berlin: Springer-Verlag, 1992.

[2] C. Edwards and S. Spurgeon, *Sliding Mode Control: Theory and Applications*. Taylor and Francis, 1998.

[3] Y. Shtessel, C. Edwards, L. Fridman, and A. Levant, *Sliding Mode Control and Observation*. Birkhauser, 2014.

[4] H. Nakamura, Y. Yamashita, and H. Nishitani, "Smooth Lyapunov functions for homogeneous differential inclusions," in *Proceedings of the 41st SICE Annual Conference*, pp. 1974–1979, 2002.

[5] V. Andrieu, L. Praly, and A. Astolfi, "Homogeneous approximation, recursive observer design, and output feedback," *SIAM Journal of Control and Optimization*, vol. 47, no. 4, pp. 1814–1850, 2008.

[6] A. Levant, "Quasi-continuous high-order sliding-mode controllers," *IEEE Transactions on Automatic Control*, vol. 50, no. 11, pp. 1812–1816, 2005.

[7] B. Ning, Q.-L. Han, and Z. Zuo, "Practical fixed-time consensus for integrator-type multi-agent systems: A time base generator approach," *Automatica*, vol. 105, pp. 406–414, 2019.

[8] A. Levant, "Sliding order and sliding accuracy in sliding mode control," *International Journal of Control*, vol. 58, no. 6, pp. 1247–1263, 1993.

[9] A. Levant, "Chattering analysis," *IEEE Transactions on Automatic Control*, vol. 55, no. 6, pp. 1380–1389, 2010.

[10] I. Boiko, *Discontinuous Control Systems : Frequency-Domain Analysis and Design*. Boston : Birkhauser, 2009.

[11] V. Acary and B. Brogliato, "Implicit Euler numerical scheme and chattering-free implementation of sliding mode systems," *Systems & Control Letters*, vol. 59, no. 5, pp. 284–293, 2010.

[12] F. Plestan, Y. Shtessel, V. Bregeault, and A. Poznyak, "New methodologies for adaptive sliding mode control," *International Journal of Control*, vol. 83, no. 9, pp. 1907–1919, 2010.

[13] V. Utkin, A. Poznyak, Y. Orlov, and A. Polyakov, "Conventional and high order sliding mode control," *Journal of the Franklin Institute*, vol. 357, pp. 10244–10261, Oct. 2020.

[14] U. Pérez-Ventura and L. Fridman, "When is it reasonable to implement the discontinuous sliding-mode controllers instead of the continuous ones? Frequency domain criteria," *International Journal of Robust and Nonlinear Control*, vol. 29, no. 3, pp. 353–374, 2019.

[15] V. Acary, B. Brogliato, and Y. Orlov, "Chattering-free digital sliding-mode control with state observer and disturbance rejection," *IEEE Transactions on Automatic Control*, vol. 57, no. 5, pp. 1087–1101, 2012.

[16] Y. Bavafa-Toosi, *Introduction to Linear Control Systems*. Elsevier, 2017.

[17] S. Boyd, E. Ghaoui, E. Feron, and V. Balakrishnan, *Linear Matrix Inequalities in System and Control Theory*. Philadelphia: SIAM, 1994.

[18] A. Polyakov, *Generalized Homogeneity in Systems and Control*. Communications and Control Engineering, Springer Nature Switzerland AG, 2020.

[19] C. Fiter, L. Hetel, W. Perruquetti, and J. Richard, "A state dependent sampling for linear state feedback," *Automatica*, vol. 48, no. 8, pp. 1860–1867, 2012.

[20] A. Levant, "On fixed and finite time stability in sliding mode control," in *IEEE Conference on Decision and Control*, (Firenze, Italy), pp. 4260–4265, 2013.

[21] O. Huber, V. Acary, and B. Brogliato, "Lyapunov stability and performance analysis of the implicit discrete sliding mode control.," *IEEE Transactions on Automatic Control*, vol. 61, no. 10, pp. 3016–3030, 2016.

[22] O. Huber, B. Brogliato, V. Acary, A. Boubakir, F. Plestan, and B. Wang, *Recent Trends in Sliding Mode Control*, ch. Experimental results on implicit and explicit time-discretization of equivalent control-based sliding mode control, pp. 207–235. IET, London, 2016.

[23] F. A. Miranda-Villatoro, B. Brogliato, and F. Castanos, "Set-valued sliding-mode control of uncertain linear systems: Continuous and discrete-time analysis," *SIAM Journal on Control and Optimization*, vol. 56, pp. 1756–1793, Jan. 2018.

[24] R. Kikuuwe, S. Yasukouchi, H. Fujimoto, and M. Yamamoto, "Proxy-based sliding mode control: A safer extension of PID position control," *IEEE Transactions on Robotics*, vol. 26, no. 4, pp. 670–683, 2010.

[25] A. Polyakov, D. Efimov, and B. Brogliato, "Consistent discretization of finite-time and fixed-time stable systems," *SIAM Journal of Control and Optimization*, vol. 57, no. 1, pp. 78–103, 2019.

[26] B. Brogliato and A. Polyakov, "Digital implementation of sliding-mode control via the implicit method: a tutorial," *International Journal of Robust and Nonlinear Control*, vol. 31, no. 9, pp. 3528–3586, 2021.

[27] B. Wang, B. Brogliato, V. Acary, A. Boubakir, and F. Plestan, "Experimental comparisons between implicit and explicit implementations of discrete-time sliding mode controllers: toward input and output chattering suppression," *IEEE Transactions on Control Systems Technology*, vol. 23, no. 5, pp. 2071–2075, 2014.

[28] O. Huber, V. Acary, B. Brogliato, and F. Plestan, "Implicit discrete-time twisting controller without numerical chattering: analysis and experimental results," *Control Engineering Practice*, vol. 46, no. 1, pp. 129–141, 2016.

[29] R. Kikuuwe, "A sliding-mode-like position controller for admittance control with bounded actuator force," *IEEE/ASME Transactions on Mechatronics*, vol. 19, no. 5, pp. 1489–1500, 2014.

[30] A. Poznyak, A. Polyakov, and V. Azhmyakov, *Attractive Ellipsoids in Robust Control*. Birkhauser, 2014.

[31] N. Kawski, "Families of dilations and asymptotic stability," in *Analysis of Controlled Dynamical Systems, Bonnard B., Bride B., Gauthier JP., Kupka I. (eds)*, pp. 285–294, 1991. Progress in Systems and Control Theory, vol 8. Birkhäuser Boston.

[32] A. Polyakov, J.-M. Coron, and L. Rosier, "On homogeneous finite-time control for linear evolution equation in Hilbert space," *IEEE Transactions on Automatic Control*, vol. 63, no. 9, pp. 3143–3150, 2018.

[33] A. Polyakov, "Sliding mode control design using canonical homogeneous norm," *International Journal of Robust and Nonlinear Control*, vol. 29, no. 3, pp. 682–701, 2018.

[34] E. Bernuau, A. Polyakov, D. Efimov, and W. Perruquetti, "Verification of ISS, iISS and IOSS properties applying weighted homogeneity," *Systems & Control Letters*, vol. 62, no. 12, pp. 1159–1167, 2013.

[35] V. Utkin, J. Guldner, and J. Shi, *Sliding Mode Control in Electro-Mechanical Systems*. CRC Press, 2009.

[36] J.-M. Coron and L. Praly, "Adding an integrator for the stabilization problem," *Systems & Control Letters*, vol. 17, no. 2, pp. 89–104, 1991.

[37] S. P. Bhat and D. S. Bernstein, "Geometric homogeneity with applications to finite-time stability," *Mathematics of Control, Signals and Systems*, vol. 17, pp. 101–127, 2005.

[38] A. Polyakov, D. Efimov, and W. Perruquetti, "Robust stabilization of MIMO systems in finite/fixed time," *International Journal of Robust and Nonlinear Control*, vol. 26, no. 1, pp. 69–90, 2016.

[39] K. Zimenko, A. Polyakov, D. Efimov, and W. Perruquetti, "Robust feedback stabilization of linear MIMO systems using generalized homogenization," *IEEE Transactions on Automatic Control*, vol. 65, no. 12, pp. 5429–5436, 2020.

[40] S. Wang, A. Polyakov, and G. Zheng, "On generalized homogenization of linear quadrotor controller," in *IEEE International Conference on Robotics and Automation (ICRA)*, pp. pp. 6190–6195, 2020. doi: 10.1109/ICRA40945.2020.9197116.

[41] G. F. Franklin, J. D. Powel, and M. L. Workman, *Digital Control of Dynamic Systems*. USA: Ellis-Kagle Press, 1998.

[42] J.-P. Aubin and A. Cellina, *Differential Inclusions. Set-Valued Maps and Viability Theory*, vol. 264 of *Grundlehren der mathematischen Wissenschaften*. Springer-Verlag Berlin Heidelberg, 1984.